Lightning electromagnetic environment in the presence of a tall grounded strike object

Yoshihiro Baba
Department of Electrical Engineering, Doshisha University, Kyoto, Japan

Vladimir A. Rakov
Department of Electrical and Computer Engineering, University of Florida, Gainesville, Florida, USA

Received 10 October 2004; revised 25 January 2005; accepted 11 February 2005; published 11 May 2005.

[1] We have analyzed and compared distance dependences of electric and magnetic fields due to a lightning strike to a tall object and due to the same lightning strike to flat ground. In both cases, lightning was represented by a transmission line energized by a lumped voltage source connected at the channel attachment point. The resultant total charge transfer to ground was the same regardless of the presence of strike object. The electric field for the strike-object case is reduced relative to the flat-ground case at closer distances from the object. If we assume, in an idealized case, that the return stroke wave front speed is equal to the speed of light, $v = c$, the current reflection coefficient at the bottom of the strike object $\rho_{bot} = 1$ (grounding impedance $Z_{gr} = 0$), and that at the top of the object for upward-propagating waves $\rho_{top} = 0$ (characteristic impedance of the object is equal to that of the channel $Z_{ob} = Z_{ch}$), the ratio of the vertical electric fields on ground for the strike-object and flat-ground cases (electric field attenuation factor) will be $d/\sqrt{(d^2 + h^2)}$, where h is the height of the strike object and d is the horizontal distance from the object. The corresponding ratio for the azimuthal magnetic field is equal to unity. We show that the ratio for either electric or magnetic field increases with decreasing ρ_{bot} ($\rho_{bot} < 1$), decreasing ρ_{top} ($\rho_{top} < 0$ except for the case of $\rho_{bot} = 0$), and decreasing v ($v < c$), and at larger distances can become greater than unity. We additionally show that the ratio of the far fields for the strike-object and flat-ground cases is given by $(1 - \rho_{top})\,(c/v + 1)/(1 + \rho_{gr})$, where ρ_{gr} is the current reflection coefficient at the lightning channel base when the channel terminates directly on ground. For realistic values of $\rho_{top} = -0.5$, $\rho_{gr} = 1$, and $v = 0.5c$, this ratio (far field enhancement factor) is equal to 2.3.

Citation: Baba, Y., and V. A. Rakov (2005), Lightning electromagnetic environment in the presence of a tall grounded strike object, *J. Geophys. Res.*, *110*, D09108, doi:10.1029/2004JD005505.

1. Introduction

[2] It is important to know the lightning electromagnetic environment in the vicinity of a tall strike object for studying lightning return-stroke processes at early times and for optimizing lightning protection means of nearby telecommunication and power distribution lines.

[3] *Rachidi et al.* [2001] have theoretically shown that the vertical electric field and azimuthal magnetic field at a distance of 2 km from a 553-m-high object struck by lightning are 2.6 times larger compared to the case when the same lightning attaches to flat ground. These calculations, based on the modified transmission line model with exponential current decay with height (MTLE) [*Nucci et al.*, 1988], were performed for a current waveform were thought to be typical for negative subsequent return strokes. *Rachidi et al.* [2001] assumed that the current propagation speed along the strike object was equal to the speed of light c, and the return stroke wave front speed was $0.63c$. They further assumed that the current reflection coefficient at the bottom of the 553-m-high object $\rho_{bot} = 0.48$ and that at the top of the object for upward-propagating waves $\rho_{top} = -0.5$ (these current reflection coefficients corresponded to, for example, a 100-Ω grounding impedance and a 900-Ω channel impedance, if the characteristic impedance of the object was assumed to be equal to 300 Ω). Note that *Rachidi et al.* [2001] employed a lumped current source that injected the same current into the channel regardless of the presence of the strike object, although the use of current source (which is characterized by infinitely large impedance) is inconsistent with the specified current reflection coefficient ($\rho_{top} = -0.5$) at the top of the object. We will show in this paper that the field enhancement effect at larger distances is observed even when this inconsistency is removed by replacing the current source by an appropriate voltage source. *Rachidi et al.* [2001] have interpreted the model-predicted increase in field magnitudes as being due to (1) the presence of two current wave fronts originating from the top of the tall object and

0148-0227/05/2004JD005505$09.00

propagating in opposite directions and (2) the relatively high speed ($v = c$) of current waves propagating along the tall object. It appears that the presence of a tall strike object serves to enhance lightning electric and magnetic fields relative to the case of strikes to flat ground. Enhancement of lightning electric and magnetic fields by a tall strike object was also discussed by *Diendorfer and Schulz* [1998], *Rakov* [2001], *Kordi et al.* [2003], and *Bermudez et al.* [2004].

[4] On the other hand, *Fisher and Schnetzer* [1994] found that a strike object appeared to reduce electric fields in its vicinity. They examined the dependence of triggered lightning electric fields on the height of strike object at Fort McClellan, Alabama. The fields were measured at distances of 9.3 and 19.3 m from the base of a metallic strike rod whose height was either 4.5 or 11 m. They observed that the leader electric fields (approximately equal to return stroke fields at such close distances) tended to be reduced as the strike object height increased.

[5] *Miyazaki and Ishii* [2004], using the Numerical Electromagnetic Code (NEC-2) [*Burke and Poggio*, 1980], examined the influence of the presence of tall strike object (60 to 240 m in height) on the associated electromagnetic fields at ground level 100 m to 500 km away from the channel. They represented the lightning channel by a vertical wire having distributed resistance (1 Ω/m) and additional distributed inductance (3 μH/m), energized by a voltage source connected between the channel and the strike object represented by a vertical perfectly conducting wire. The voltage source had internal resistance of 300 Ω. Grounding resistance of the strike object was assumed to be 30 Ω, and ground conductivity was set to 0.003 S/m. The ratio of the calculated vertical electric field due to a lightning strike to a tall object of 60 to 240 m in height to that due to the same strike to flat ground is smaller than unity at horizontal distances of 100 to 600 m from the channel, but is larger than unity beyond 600 m. The ratio reaches its peak around several kilometers from the channel, and then begins to decrease with increasing horizontal distance. Miyazaki and Ishii noted that this decrease was due to the propagation effects (attenuation of electromagnetic waves as they propagate over lossy ground).

[6] In this paper, we will examine the distance dependences of electric and magnetic fields due to lightning strikes to the top of a tall grounded object and compare those fields with their counterparts for strikes to flat ground. In doing so, we will represent both the lightning channel and the strike object by lossless, uniform transmission lines energized at their junction by a lumped voltage source [*Baba and Rakov*, 2005] (in fact, each of the two vertical conductors, lightning channel or strike object, can be viewed as the return path for the other [*Thottappillil et al.*, 2001]). In specifying the source, we will use the current waveform proposed by *Nucci et al.* [1990], which is thought to be typical for lightning subsequent return strokes.

[7] The structure of the paper is as follows. In section 2, we present expressions for current along the tall strike object and along the lightning channel, to be used in calculating electric and magnetic fields in the vicinity of the strike object. In section 3, using these expressions, we calculate vertical electric fields and azimuthal magnetic fields on a perfectly conducting ground due to a lightning strike to a 100-m-high object under the following idealized conditions: There is perfect current reflection at the bottom of the object ($\rho_{bot} = 1$), there is no reflection at the top of the object for upward-propagating current waves ($\rho_{top} = 0$), and the return stroke wave front speed is equal to the speed of light ($v = c$). We compare the resultant fields with those due to the same strike to flat ground. In sections 4, 5, and 6, we examine influences on the distance dependences of fields due to a lightning strike to the tall object, relative to those due to the same strike to flat ground, of the current reflection coefficient at the bottom of the strike object (ρ_{bot} = 1, 0.7, and 0), current reflection coefficient (for upward-propagating waves) at the top of the object (ρ_{top} = 0, −0.5, and −1), and return stroke wave front speed ($v = c$ and $0.5c$), respectively. Additionally, we consider the influence of object height and lightning return stroke current risetime. In section 7, we compare the results obtained in this paper with experimental data, and in section 8, with those obtained using other modeling methods. In Appendix A, we show that lightning strikes to a tall object and to flat ground considered in this paper are associated with the same charge transfer to ground. In Appendix B, we derive an equation for the far field enhancement factor due to the presence of a tall strike object using current expressions presented in section 2.

2. Distribution of Current Along the Tall Strike Object and Along the Lightning Channel

[8] In this section, we present expressions, derived by *Baba and Rakov* [2005], for current along the tall strike object and along the lightning channel, to be used in the following sections in calculating electric and magnetic fields in the vicinity of the strike object. Figure 1a shows a transmission line representation of lightning strike to a tall grounded object, comprising two lossless uniform transmission lines representing the lightning channel (whose characteristic impedance is Z_{ch}) and the tall strike object of height h (whose characteristic impedance is Z_{ob}), a lumped grounding impedance (Z_{gr}), and a lumped voltage source that generates a voltage waveform $V_0(h, t) = Z_{ch}I_{sc}(h, t)$, where $I_{sc}(h, t)$ is the lightning short-circuit current. The lightning short-circuit current, $I_{sc}(h, t)$, is defined [*Baba and Rakov*, 2005] as the lightning current that would be measured at an ideally grounded object ($Z_{gr} = 0$ or $Z_{gr} \ll Z_{ch}$) of negligible height ($h \approx 0$). The current propagation speed along the strike object is assumed to be equal to the speed of light c and that along the lightning channel to be equal to v, the return stroke wave front speed. The current reflection coefficient at the bottom of the tall object (ρ_{bot}) and the current reflection coefficient at the top of the object for upward-propagating waves (ρ_{top}) are given by

$$\rho_{bot} = \frac{Z_{ob} - Z_{gr}}{Z_{ob} + Z_{gr}}.$$

$$\rho_{top} = \frac{Z_{ob} - Z_{ch}}{Z_{ob} + Z_{ch}}. \quad (1)$$

Current distributions, $I(z', t)$, along the tall object ($0 \le z' \le h$) and along the lightning channel ($z' \ge h$), for the

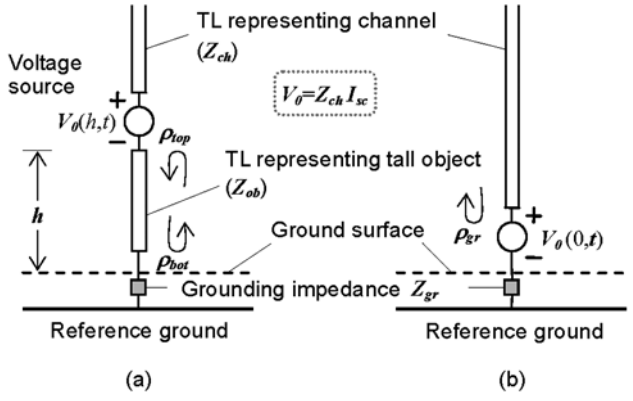

Figure 1. Lightning strikes (a) to a tall grounded object of height h and (b) to flat ground, represented by lossless transmission lines connected in series with a lumped voltage source generating an arbitrary voltage waveform, $V_0(h, t) = Z_{ch}I_{sc}(h, t)$ or $V_0(0, t) = Z_{ch}I_{sc}(0, t)$, and a lumped grounding impedance (Z_{gr}). Z_{ch} is the characteristic impedance of the transmission line representing the lightning channel, and Z_{ob} is that representing the tall strike object; ρ_{top} is the current reflection coefficient at the top of the tall object for upward-propagating waves, and ρ_{bot} is the current reflection coefficient at the bottom of the tall object; ρ_{gr} is the current reflection coefficient at the channel base (ground) in the absence of a strike object.

configuration shown in Figure 1a, are given by

Along the strike object

$$I(z',t) = \frac{1-\rho_{top}}{2}\sum_{n=0}^{\infty}\left[\begin{array}{l}\rho_{bot}^{n}\rho_{top}^{n}I_{sc}\left(h,t-\dfrac{h-z'}{c}-\dfrac{2nh}{c}\right)\\ +\rho_{bot}^{n+1}\rho_{top}^{n}I_{sc}\left(h,t-\dfrac{h+z'}{c}-\dfrac{2nh}{c}\right)\end{array}\right] \quad 0\le z'\le h \tag{2a}$$

Along the lightning channel

$$I(z',t) = \frac{1-\rho_{top}}{2}\cdot\left[\begin{array}{l}I_{sc}\left(h,t-\dfrac{z'-h}{v}\right)\\ +\displaystyle\sum_{n=1}^{\infty}\rho_{bot}^{n}\rho_{top}^{n-1}\left(1+\rho_{top}\right)I_{sc}\left(h,t-\dfrac{z'-h}{v}-\dfrac{2nh}{c}\right)\end{array}\right] \quad z'\ge h, \tag{2b}$$

where n is an index representing the successive multiple reflections occurring at the two ends of the strike object. Equations (2a) and (2b) are the same as equations (10a) and (10b) of *Baba and Rakov* [2005], except v_{ref}, the speed of current waves reflected from ground and then transmitted into the channel, in equation (10b) is replaced by v in equation (2b). Rationale for replacing v_{ref} with v is discussed by *Baba and Rakov* [2005]. Equations (2a) and (2b) show that two current waves of the same magnitude, $(1 - \rho_{top})I_{sc}(h, t)/2$, are initially injected downward, into the tall object, and upward, into the channel. Note that Equation (2a) is the same as equation (25) of *Rachidi et al.* [2002], who used a distributed-shunt-current-source representation of the lightning channel, and the structure of equation (2b) is the same as that of equation (24) of *Rachidi et al.* [2002], although their equations are written in terms of the so-called "undisturbed" (matched-conditions) current, $I_{mc}(h, t) = I_{sc}(h, t)/2$, as discussed by *Baba and Rakov* [2005].

[9] The current distribution, $I(z', t)$, along the lightning channel for the case of strike to flat ground (see Figure 1b), is given by [*Baba and Rakov*, 2005]

$$I(z',t) = \frac{1+\rho_{gr}}{2}I_{sc}\left(0,t-\frac{z'}{v}\right), \tag{3}$$

where $I_{sc}(0, t)$ is the lightning short-circuit current (same as $I_{sc}(h, t)$ in Equations (2a) and (2b) but injected at $z' = 0$ instead of $z' = h$), and ρ_{gr} is the current reflection coefficient at the channel base (ground). Equation for ρ_{gr} (although no downward-propagating current wave would be present along the uniform transmission line representing the lightning channel shown in Figure 1b) is given by

$$\rho_{gr} = \frac{Z_{ch}-Z_{gr}}{Z_{ch}+Z_{gr}}. \tag{4}$$

Note that equation (2b) reduces to equation (3) and equation (2a) reduces to equation (3) with $z' = 0$ when h approaches zero [*Baba and Rakov*, 2005]. The total charge transfer to ground, calculated integrating current given by equation (2a) at $z' = 0$, is the same as that calculated integrating current given by equation (3) at $z' = 0$ (see Appendix A). Therefore current distributions for the case of strikes to a tall object (Equations (2a) and (2b)) and for the case of strikes to flat ground (equation (3)) correspond to the same lightning discharge, as required for examining the influence of the strike object. On the other hand, currents injected into the lightning channel in these two cases are generally not the same, as discussed next.

[10] It follows from equations (2b) and (3) that currents injected into the lightning channel from the source for configurations shown in Figures 1a and 1b are given by $I = (1 - \rho_{top})I_{sc}/2$ and $I = (1 + \rho_{gr})I_{sc}/2$, respectively. These two currents are different, unless $\rho_{top} = 0$ and $\rho_{gr} = 0$ (matched conditions at the position of the source) or $\rho_{top} = -\rho_{gr}$ ($Z_{ob} = Z_{gr}$; i.e. $\rho_{bot} = 0$). Both situations are physically unrealistic, since typically $\rho_{gr} = 1$ ($Z_{gr} \ll Z_{ch}$ and $Z_{gr} \ll Z_{ob}$). If one forced the current injected into the lightning channel from the source in configuration shown in Figure 1a to be the same as that in configuration shown in Figure 1b (by setting the magnitude of the voltage source to $V_0(h, t) = (1 + \rho_{gr})/(1 - \rho_{top})xZ_{ch}I_{sc}(h, t)$ instead of $Z_{ch}I_{sc}(h, t)$, while keeping $V_0(0, t) = Z_{ch}I_{sc}(0, t)$), then for realistic values of $\rho_{gr} = 1$ and $\rho_{top} = -0.5$ the total charge transfer to ground for the tall-strike-object case would be 1.3 times larger than that for the flat-ground case.

[11] Table 1 shows the magnitudes of current waves injected by the source into the channel, in terms of the lightning short-circuit current, for strikes to a tall object (Figure 1a) and to flat ground (Figure 1b). The current magnitudes are calculated using equations (2b) and (3), with the resultant charge transfer to ground being the same in

Table 1. Magnitudes, I, of Current Waves Injected Into the Lightning Channel From the Source for the Configurations Shown in Figures 1a and 1b, as a Function of the Lightning Short-Circuit Current, I_{sc}, for Different Sets of Current Reflection Coefficients, ρ_{top}, ρ_{bot}, and ρ_{gr}

Current Reflection Coefficients	Strike to Tall Object[a]	Strike to Flat Ground[b]
$\rho_{top} = 0$, $\rho_{bot} = 1$, $\rho_{gr} = 1$ ($Z_{gr} = 0\ \Omega$, $Z_{ob} = Z_{ch}$)	$0.5I_{sc}$	I_{sc}
$\rho_{top} = 0$, $\rho_{bot} = 0.9$, $\rho_{gr} = 0.9$ ($Z_{gr} = 50\ \Omega$, $Z_{ob} = Z_{ch} = 900\ \Omega$)	$0.5I_{sc}$	$0.95I_{sc}$
$\rho_{top} = -0.5$, $\rho_{bot} = 1$, $\rho_{gr} = 1$ ($Z_{gr} = 0\ \Omega$, $Z_{ob} = 300\ \Omega$, $Z_{ch} = 900\ \Omega$)	$0.75I_{sc}$	I_{sc}
$\rho_{top} = -0.5$, $\rho_{bot} = 0$, $\rho_{gr} = -\rho_{top} = 0.5$ ($Z_{gr} = Z_{ob} = 300\ \Omega$, $Z_{ch} = 3Z_{ob} = 900\ \Omega$)	$0.75I_{sc}$	$0.75I_{sc}$

[a]Figure 1a: $I = (1 - \rho_{top})I_{sc}/2$.
[b]Figure 1b: $I = (1 + \rho_{gr})I_{sc}/2$.

both cases. As expected, the injected current magnitude depends on Z_{gr} and Z_{ch} for strikes to flat ground (although usually $Z_{gr} \ll Z_{ch}$ in which case the injected current is equal to I_{sc}) and on Z_{ob} and Z_{ch} for strikes to the tall object.

3. Basic Case ($\rho_{bot} = \rho_{gr} = 1$, $\rho_{top} = 0$, $v = c$)

3.1. Comparison of a Lightning Strike to a Tall Object With That to Flat Ground

[12] In this section, we compare the vertical electric field and azimuthal magnetic field at ground level due to a lightning strike to a tall object of height $h = 100$ m with their counterparts due to the same strike to flat ground. We consider here an idealized situation in which the current reflection coefficient at the top of the tall object is $\rho_{top} = 0$ (no reflection and perfect transmission; $Z_{ob} = Z_{ch}$) and the current reflection coefficient at the bottom of the object is $\rho_{bot} = 1$ (perfect reflection; $Z_{gr} = 0\ \Omega$). In the case of lightning strike to flat ground, we assume that the current reflection coefficient at the channel base (ground) is $\rho_{gr} = 1$ (perfect reflection; $Z_{gr} = 0\ \Omega$). Also, we assume here that the return-stroke speed is equal to the speed of light, $v = c$, which will greatly simplify our analysis. This is our basic case. We will examine the influences of variation in ρ_{bot} (and ρ_{gr}), ρ_{top}, and v on computed fields in sections 4, 5, and 6, respectively.

[13] Figure 2a shows vertical electric fields on perfectly conducting ground for a lightning strike to the 100-m-high object, at horizontal distances of $d = 30$, 60, 100, and 300 m from the object. The electric fields (including the electrostatic, induction, and radiation components) were calculated using the expression for the electric field due to an infinitesimal current dipole [*Uman et al.*, 1975; *Thottappillil et al.*, 1998] that was integrated over the radiating sections of the channel and the strike object. The presence of ground was accounted for using the image theory. Figure 2b shows the corresponding electric fields calculated for the same lightning strike to flat ground. Figures 3a and 3b are similar to Figures 2a and 2b, respectively, but for azimuthal magnetic fields (including the induction and radiation components). Note that vertical scales in Figures 2a and 2b are different, while in Figures 3a and 3b they are the same. Current distributions along the 100-m-high object and along the lightning channel, used in calculating fields shown in Figures 2a and 3a, are given by Equations (2a) and (2b), and current distribution along the lightning channel used in calculating fields shown in Figures 2b and 3b is given by equation (3). Since ρ_{top} is assumed to be equal to 0 ($Z_{ob} = Z_{ch}$), and ρ_{bot} to be equal to 1 ($Z_{gr} = 0$), the magnitude of current waves injected initially into the tall object and into the channel in configuration of Figure 1a is $0.5I_{sc}(h, t)$, and that of the current wave injected into the channel in configuration of Figure 1b is $I_{sc}(0, t)$. As noted in section 1, we used a current waveform proposed by *Nucci et al.* [1990] as the lightning short-circuit current, $I_{sc}(h, t)$ or $I_{sc}(0, t)$. Note that the electric and magnetic field waveforms in Figures 2 and 3 have identical shapes that are the same as the current waveshape. This is a result of our assumptions ($\rho_{top} = 0$, $\rho_{bot} = 1$, and $v = c$), under which two spherical TEM waves are formed, as further discussed in section 3.2.

[14] As seen in Figures 2a and 2b, at distances ranging from 30 to 300 m the magnitude of the vertical electric field due to a lightning strike to the top of the 100-m-high object is smaller than that due to the same strike to flat ground. Although no field waveforms are shown here, as the distance increases beyond 300 m, the ratio of electric field magnitudes for these two cases approaches unity. The reduction of lightning electric field in close proximity of

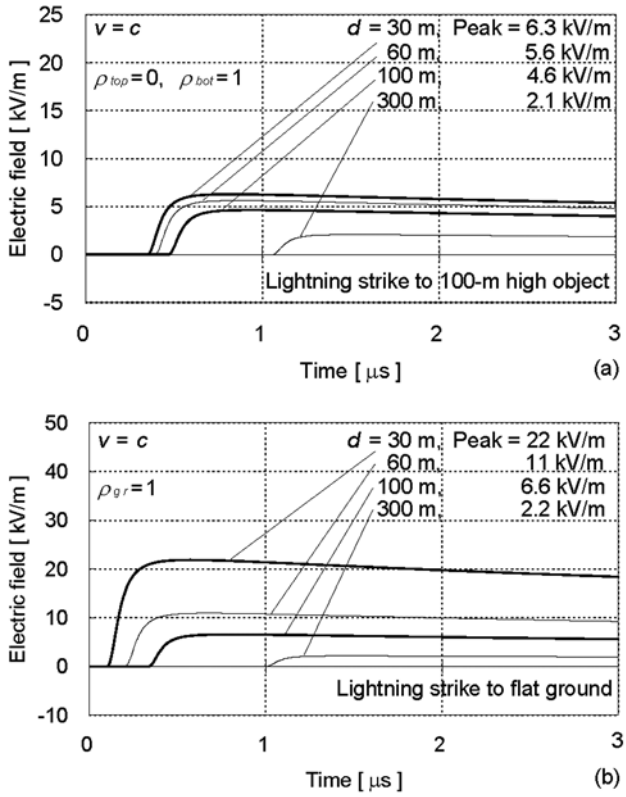

Figure 2. Basic case ($\rho_{bot} = \rho_{gr} = 1$, $\rho_{top} = 0$, $v = c$). Vertical electric field waveforms (a) due to a lightning strike to 100-m-high object and (b) due to the same lightning strike to flat ground, at horizontal distances of $d = 30$, 60, 100, and 300 m from the lightning channel.

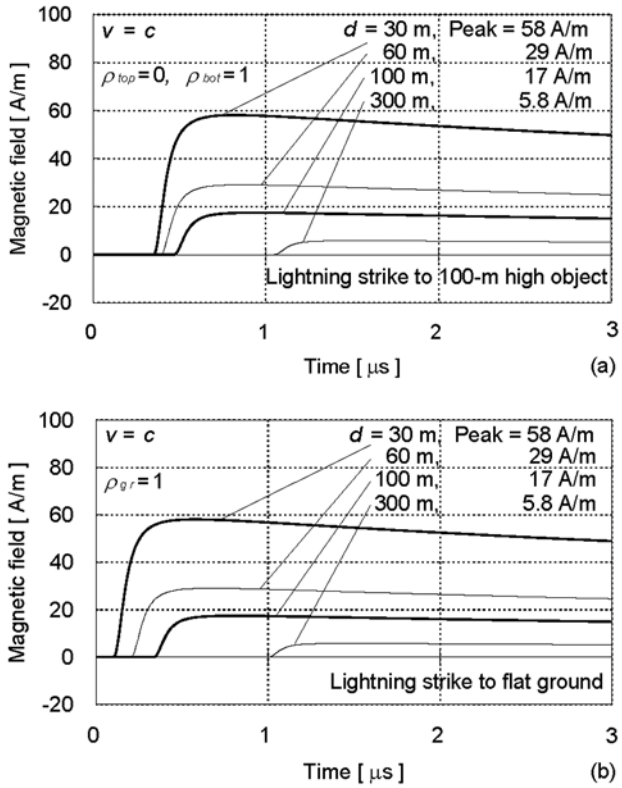

Figure 3. Same as Figure 2, but for the azimuthal magnetic field.

grounded strike object might be regarded as the electric field shielding effect of the object.

[15] As seen in Figures 3a and 3b, at any distance the azimuthal magnetic field due to a lightning strike to the 100-m-high object is identical to that in the absence of the object (due to a strike to flat ground).

[16] We will further discuss distance dependences of electric and magnetic fields for the strike-object and flat-ground cases, as well as of field ratios (electric field attenuation factors), in section 3.2.

3.2. Analysis of Distance Dependences of the Ratios of Electric and Magnetic Fields for Tall-Object and Flat-Ground Cases

[17] In this section, we utilize the ideal transmission line theory developed by *Thottappillil et al.* [2001], which will allow us to obtain easy-to-analyze analytical expressions for lightning electric and magnetic fields. These expressions are valid for the case of (1) ideal grounding ($Z_{gr} = 0$), (2) no reflection at the junction between the lightning channel and tall strike object ($Z_{ch} = Z_{ob}$), and (3) propagation of all current waves, both along the strike object and along the channel, at the speed of light. Clearly, these are the same assumptions we made in formulating our basic case. In sections 4, 5, and 6, we will examine the influence of each of these three assumptions on the inferences regarding the lightning electromagnetic environment in the vicinity of a tall strike object made in this section.

[18] Additionally, the analytical field expressions used in this section require that both the lightning channel and the strike object are approximated by conductors of vanishing radius [*Thottappillil et al.*, 2001]. This latter idealization is discussed by *Kordi et al.* [2002], *Thottappillil and Uman* [2002], and *Baba and Rakov* [2003]. Since we assumed $Z_{gr} = 0$ (ideal grounding), we can use the method of images to replace the configuration shown in Figure 1a by a vertical wire of infinite extent that is energized by two voltage sources, as shown in Figure 4a. The configuration shown in Figure 4a in turn can be replaced by its equivalent involving two infinitely long vertical wires, each energized by a single source, as shown in Figure 4b. Note that the two vertical wires shown in Figure 4b are actually collocated and shown separated for illustrative purpose only. Each source generates two current waves propagating without attenuation or distortion in the upward and downward directions. Since the current wave speed is assumed to be equal to the speed of light, the resultant electromagnetic field structure is spherical TEM [e.g., *Thottappillil et al.*, 2001; *Kordi et al.*, 2002; *Baba and Rakov*, 2003], and we can apply the analytical expressions for TEM-wave electric and magnetic fields derived by *Thottappillil et al.* [2001]. Total fields due to both wires shown in Figure 4b, corresponding to the configuration shown in Figure 1a (with $Z_{gr} = 0$ and $Z_{ch} = Z_{ob}$), will be obtained using the principle of superposition.

[19] The vertical electric field, E_z, on the reference ground plane at horizontal distance d from the wire energized at height h (left wire in Figure 4b) is given by [*Thottappillil et al.*, 2001]

$$E_z(d,t) = E_\theta(d,t)\sin\theta = \frac{1}{2\pi\varepsilon_0 c\sqrt{d^2+h^2}}\,0.5I_{sc}\left(h, t-\frac{\sqrt{d^2+h^2}}{c}\right), \quad (5)$$

where $E_\theta(d, t)$ is the θ-component of the electric field, ε_0 is the permittivity of vacuum, $\sqrt{(d^2 + h^2)}$ is the radial distance

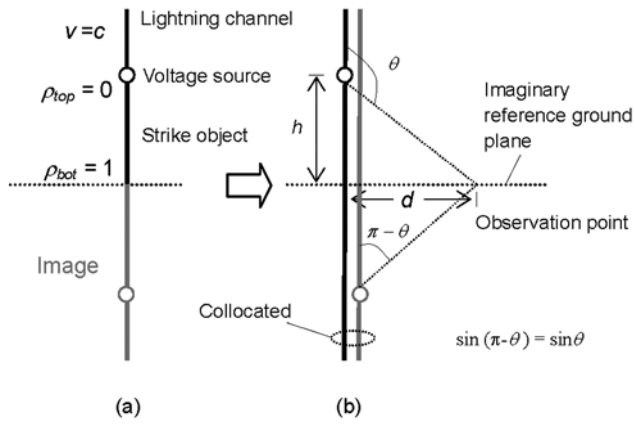

Figure 4. Approximation of the configuration shown in Figure 1a in the case of $\rho_{bot} = 1$ and $\rho_{top} = 0$ ($Z_{gr} = 0\ \Omega$, $Z_{ob} = Z_{ch}$). (a) Vertical wire of zero radius and infinite longitudinal extent, energized by two voltage sources. The position of the imaginary reference ground plane is indicated by a horizontal dotted line. (b) Superposition of two wires, each energized by a single, zero-impedance source. Each wire produces a spherical TEM wave. Geometrical parameters used in deriving electric and magnetic field equations are shown.

from the source (at the top of the strike object) to the observation point, and θ is the angle between the vertical wire and the straight line passing through both the source and the observation point. Current injected into the wire in this case is $0.5I_{sc}$, as discussed above (see Table 1). Note that equation (5) gives the total electric field which is the sum of the electrostatic, induction, and radiation components [*Thottappillil et al.*, 2001].

[20] The wire whose excitation point is below the reference ground plane (right wire in Figure 4b) produces, due to symmetry, the same vertical electric field on the reference ground plane as the other wire whose excitation point is above the reference ground plane. Hence the total vertical electric field, E_{z_tall}, on ground at horizontal distance d from the strike object of height h is given by

$$E_{z\_tall}(d,t) = \frac{1}{2\pi\varepsilon_0 c\sqrt{d^2+h^2}} I_{sc}\left(h, t - \frac{\sqrt{d^2+h^2}}{c}\right). \quad (6)$$

Equation (6) shows that the vertical electric field in the vicinity of a tall object is inversely proportional to the radial distance, $\sqrt{(d^2 + h^2)}$, from the source at the top of the tall object to the observation point. The inverse dependence of the total electric field on the radial distance, $\sqrt{(d^2 + h^2)}$, from the source at height h, not expected for a vertical lightning channel, is due to the assumption $v = c$.

[21] For the case of strike to flat ground, equation for the vertical electric field can be obtained by setting $h = 0$ in equation (6) and is given by

$$E_{z\_flat}(d,t) = \frac{1}{2\pi\varepsilon_0 cd} I_{sc}\left(0, t - \frac{d}{c}\right). \quad (7)$$

Equation (7) shows that the vertical electric field (including its electrostatic, induction, and radiation components) on ground, due to a lightning strike to flat ground is inversely proportional to horizontal distance d from the channel, as expected for a spherical TEM wave whose source is located on the ground plane.

[22] The ratio E_{z_tall} to E_{z_flat} given by equations (6) and (7), respectively, is

$$\frac{E_{z\_tall}(d,t)}{E_{z\_flat}(d,t)} = \frac{d}{\sqrt{d^2+h^2}} = \frac{d/h}{\sqrt{(d/h)^2+1}} \le 1. \quad (8)$$

As expected, the ratio, which can be viewed as the electric field attenuation factor due to the presence of the strike object, is equal to unity when $h = 0$ or $d^2 \gg h^2$. Figure 5 shows the ratio E_{z_tall}/E_{z_flat} as a function of d/h, calculated using equation (8). E_{z_tall} is much less than E_{z_flat} at $d \ll h$, one half of E_{z_flat} at $d = h/\sqrt{3}$ (= 60 m for h = 100 m), and nearly equal to E_{z_flat} beyond $d = 3h$ to $4h$.

[23] The azimuthal magnetic field, H_φ, at the reference ground plane at horizontal distance d from the left wire energized at height h (see Figure 4b) is given by

$$H_\varphi(d,t) = \frac{1}{2\pi d} 0.5 I_{sc}\left(h, t - \frac{\sqrt{d^2+h^2}}{c}\right). \quad (9)$$

The wire whose excitation point is below the reference ground plane (right wire in Figure 4b) produces the same azimuthal magnetic field on the reference ground plane as the other wire whose excitation point is above the reference ground plane. Hence the total azimuthal magnetic field, H_{φ_tall}, on ground at horizontal distance d from the strike object is given by

$$H_{\varphi\_tall}(d,t) = \frac{1}{2\pi d} I_{sc}\left(h, t - \frac{\sqrt{d^2+h^2}}{c}\right). \quad (10)$$

Equation (10) shows that the azimuthal magnetic field in the vicinity of a tall object is inversely proportional to the horizontal distance d from the object.

[24] Setting $h = 0$ in equation (10) we obtain the corresponding equation for the case of strike to flat ground,

$$H_{\varphi\_flat}(d,t) = \frac{1}{2\pi d} I_{sc}\left(0, t - \frac{d}{c}\right). \quad (11)$$

The ratio H_{φ_tall} to H_{φ_flat} given by equations (10) and (11), respectively, is

$$\frac{H_{\varphi\_tall}(d,t)}{H_{\varphi\_flat}(d,t)} = 1. \quad (12)$$

Equation (12), plotted as a function of d/h in Figure 5, shows that H_{φ_tall} is the same as H_{φ_flat} regardless of distance or strike object height.

[25] Note that one can calculate the same electric field waveforms as shown in Figures 2a and 2b, using equations (6) and (7), respectively, and the same magnetic field waveforms as shown in Figures 3a and 3b using equations (10) and (11), respectively. This confirms that equations (6), (7), (10), and (11) are exact, provided that the assumptions made in deriving these analytical equations are valid. We will examine these assumptions in sections 4, 5, and 6.

[26] In summary, the vertical electric field is strongly attenuated at small distances from the strike object (relative to the fields due to the same strike to flat ground). This is consistent with the boundary condition at the junction between electrically long strike object and perfectly conducting ground, which requires that the charge density vanishes (while current doubles) at $z' = 0$. On the other hand, at large distances, the vertical electric field is essentially not influenced by the presence of the strike object. The azimuthal magnetic field is the same regardless of the presence of the strike object. We will show in sections 4, 5, and 6 that both electric and magnetic fields can be enhanced (electric fields at larger distances only) by the presence of the tall strike object, when the assumptions made in this section are relaxed.

4. Influence of Imperfect Current Reflection From Ground

[27] Here, we examine the influence of the assumption $\rho_{bot} = \rho_{gr} = 1$ made in the basic case (see section 3), assuming $\rho_{bot} = \rho_{gr} = 0.7$ in section 4.1 and considering three values of ρ_{bot}, 1, 0.7, and 0, in section 4.2.

4.1. Comparison of a Lightning Strike to a Tall Object With That to Flat Ground

[28] In this section, we compare the vertical electric field and azimuthal magnetic field at ground level due to a

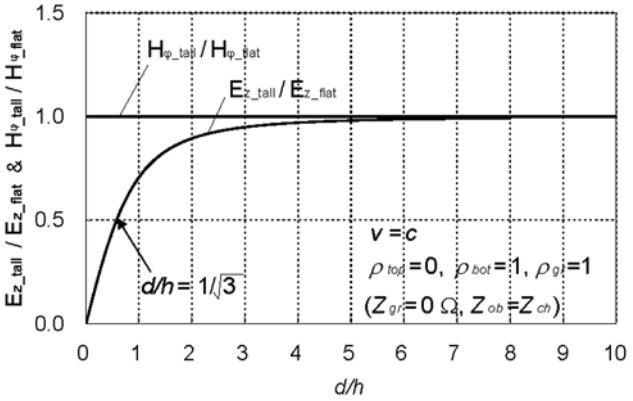

Figure 5. Ratios E_{z_tall}/E_{z_flat} and $H_{\varphi\_tall}/H_{\varphi\_flat}$, each as a function of d/h, calculated using equations (8) and (12), respectively.

lightning strike to 100-m-high object with those due to the same strike to flat ground, assuming that $\rho_{bot} = \rho_{gr} = 0.7$ (corresponding, for example, to $Z_{gr} = 50\ \Omega$ and $Z_{ob} = Z_{ch} = 300\ \Omega$). Note that *Janischewskyj et al.* [1996], from their analysis of five current waveforms measured 474 m above ground on the 553-m CN tower, inferred ρ_{bot} to vary from 0.34 to 0.43, and *Fuchs* [1998], from 13 simultaneous current measurements at the top and bottom of the 160-m

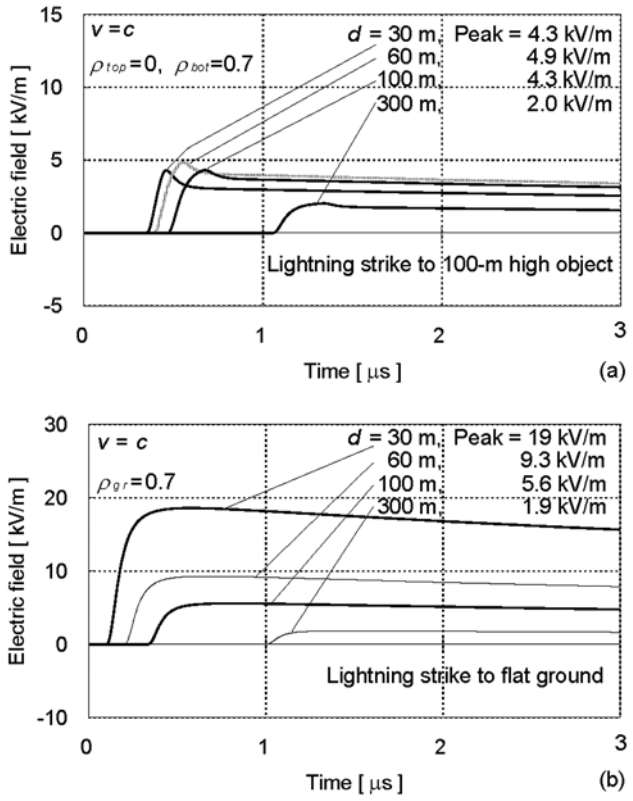

Figure 6. Imperfect ground reflection case ($\rho_{bot} = \rho_{gr} = 0.7$, $\rho_{top} = 0$, $v = c$). Vertical electric field waveforms (a) due to a lightning strike to 100-m high object and (b) due to the same lightning strike to flat ground, at horizontal distances of d = 30, 60, 100, and 300 m from the lightning channel.

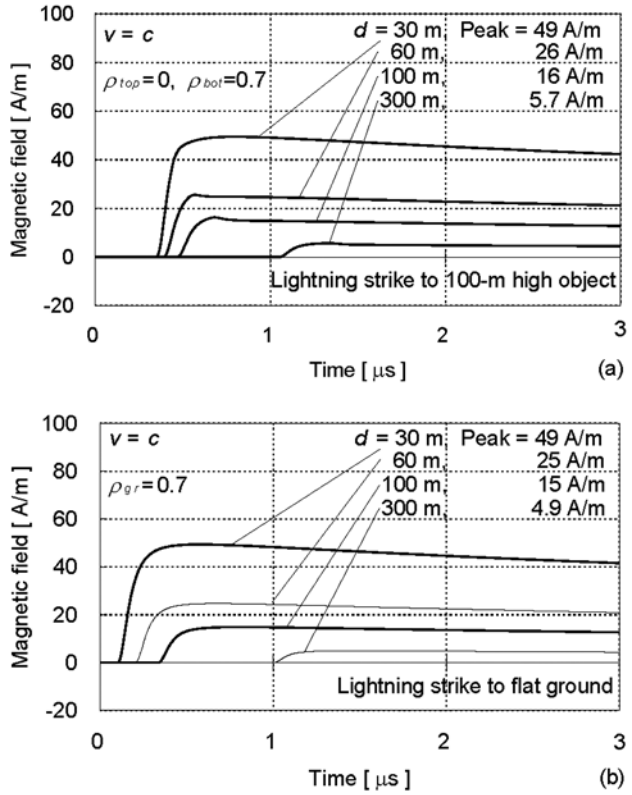

Figure 7. Same as Figure 6, but for the azimuthal magnetic field.

Peissenberg tower, found ρ_{bot} to vary from 0.64 to 0.81. All other assumptions remain the same as in section 3.

[29] Figure 6a shows vertical electric fields on perfectly conducting ground for a lightning strike to the 100-m-high object at horizontal distances of d = 30, 60, 100, and 300 m from the object. Figure 6b shows the corresponding electric fields for the same lightning strike to flat ground. Figures 7a and 7b are similar to Figures 6a and 6b, respectively, but for azimuthal magnetic fields. The fields were calculated in the same manner as in section 3.1. Note that vertical scales in Figures 6a and 6b are different, while in Figures 7a and 7b they are the same.

[30] As seen in Figures 6a and 6b, in the case of $\rho_{bot} = \rho_{gr} = 0.7$, the peak of the vertical electric field due to a lightning strike to the 100-m-high object is smaller than that due to the same strike to flat ground at d = 30 to 100 m, but larger at d = 300 m. This indicates that imperfect ground reflection serves to enhance electric fields at larger distances from the strike object, the effect not observed when $\rho_{bot} = \rho_{gr} = 1$ (see Figure 5). As seen in Figure 6a, the peak of vertical electric field calculated for $\rho_{bot} = 0.7$ increases and then decreases with increasing horizontal distance from the strike object: 4.3, 4.9, 4.3, and 2.0 kV/m at d = 30, 60, 100, and 300 m, respectively. Also, the electric field peak in the case of $\rho_{bot} = 0.7$ is smaller than in the case of $\rho_{bot} = 1$ (see Figure 2a), by 32, 14, 7, and 2% at d = 30, 60, 100, and 300 m, respectively. The latter result indicates that the influence of imperfect current reflection from ground is more significant at closer distances.

[31] As seen in Figures 7a and 7b, in the case of $\rho_{bot} = \rho_{gr} = 0.7$, the peak of the azimuthal magnetic field due to a lightning strike to the 100-m-high object is larger than that due to the same strike to flat ground at d = 60 to 300 m, while being the same at d = 30 m. Thus, similar to electric fields, imperfect ground reflection serves to enhance magnetic fields at larger distances from the strike object. The peak of azimuthal magnetic field calculated for ρ_{bot} = 0.7 monotonically decreases with increasing the horizontal distance from the strike object: 49, 26, 16, and 5.7 A/m at d = 30, 60, 100, and 300 m, respectively. Similar to the electric field peak, the magnetic field peak is smaller in the case of ρ_{bot} = 0.7 (see Figure 7a) than in the case of ρ_{bot} = 1 (see Figure 3a), by 15, 12, 7, and 2% at d = 30, 60, 100, and 300 m, respectively.

4.2. Analysis of Distance Dependences of the Ratios of Electric and Magnetic Fields for Tall-Object and Flat-Ground Cases

[32] In this section, we further discuss the influence of the current reflection coefficient at ground on distance dependences of electric and magnetic fields for the strike-object and flat-ground cases. In doing so, we will use a configuration that involves four appropriately energized vertical wires generating TEM waves. The total electric and magnetic fields will be obtained as a superposition of these TEM waves.

[33] *Rakov et al.* [1995] considered the lightning M-component electric field as a superposition of field contributions from a downward-progressing incident current wave and an upward-progressing current wave reflected from ground. We employ their approach below in deriving equations for electric and magnetic fields due to a lightning strike to the 100-m-high object, assuming no reflection at the top of the strike object (ρ_{top} = 0) and imperfect current reflection at the bottom of the object ($\rho_{bot} < 1$). We refer to current waves, propagating upward and downward from the top of the object, $0.5I_{sc}(h, t - (z' - h)/v)$ and $0.5I_{sc}(h, t - (h - z')/c)$, respectively, as incident current waves, and to an upward-propagating current wave reflected from the bottom of the object (from the ground), $0.5\rho_{bot}I_{sc}(h, t - (h + z')/c)$, as a reflected current wave. Equations (6) and (10) give total electric and magnetic fields, respectively, including their incident and reflected components for the case of ρ_{bot} = 1. In order to employ an arbitrary value of ρ_{bot}, we first eliminate the reflected-wave contributions from equations (6) and (10) and then add a contribution from the reflected wave corresponding to the new value of ρ_{bot}. This can be accomplished by modifying the two-wire configuration shown in Figure 4b to include two additional wires as shown in Figure 8. Note that these four wires are collocated and shown separated for illustrative purpose only. Wires 1 and 2 in Figure 8 are the same as the two wires in Figure 4b, while wires 3 and 4, energized at the reference ground plane, cancel the perfect ground reflection and add an imperfect ground reflection, respectively. Indeed, wire 3 injects current waves, $I_c(0, t) = -0.5I_{sc}(h, t - h/c)$, which cancel the perfectly reflected current waves produced by wires 1 and 2. Thus wires 1, 2, and 3 produce incident current waves, which correspond to the case of ρ_{bot} = 0 (matched conditions at the bottom of the strike object). Wire 4 produces current waves reflected (imperfectly) from ground, $I_{ref}(0, t) = 0.5\rho_{bot}I_{sc}(h, t - h/c)$. Note that wires 3 and 4 produce waves that cancel each other if ρ_{bot} = 1 (perfect ground reflection case).

[34] As stated above, wires 1, 2, and 3 in Figure 8 represent incident current waves that are absorbed at ground level, and wire 4 represents reflected current waves. Thus, from equation (6) and equation (5) with h = 0 and noting that $I_{sc}(0, t - d/c) = I_{sc}(h, t - h/c - d/c)$, the vertical electric field at the reference ground plane is given by

$$E_{z\_tall}(d,t) = \frac{1}{2\pi\varepsilon_0 c\sqrt{d^2+h^2}} I_{sc}\left(h, t - \frac{\sqrt{d^2+h^2}}{c}\right) - \frac{1}{2\pi\varepsilon_0 cd} 0.5 I_{sc}\left(h, t - \frac{h}{c} - \frac{d}{c}\right) + \frac{1}{2\pi\varepsilon_0 cd} 0.5\rho_{bot} I_{sc}\left(h, t - \frac{h}{c} - \frac{d}{c}\right), \quad (13)$$

where the first term which varies as $1/\sqrt{(d^2 + h^2)}$ is the field due to wires 1 and 2 in Figure 8, the second and third terms which vary as $1/d$ are the fields due to wires 3 and 4, respectively. If ρ_{bot} = 1, the total field is given by the first term of equation (13), as in the basic case considered in section 3. If h = 0 (the case of strike to flat ground), equation (13) reduces to

$$E_{z\_flat}(d,t) = \frac{1}{2\pi\varepsilon_0 cd} I_{sc}\left(0, t - \frac{d}{c}\right) - \frac{1}{2\pi\varepsilon_0 cd}(1-\rho_{bot}) 0.5 I_{sc}\left(0, t - \frac{d}{c}\right) = \frac{1+\rho_{bot}}{2}\frac{1}{2\pi\varepsilon_0 cd} I_{sc}\left(0, t - \frac{d}{c}\right). \quad (14)$$

If ρ_{bot} = 1, equation (14) reduces to equation (7).

[35] Similarly, the azimuthal magnetic fields due to strikes to a tall object and to flat ground are given by

$$H_{\varphi\_tall}(d,t) = \frac{1}{2\pi d} I_{sc}\left(h, t - \frac{\sqrt{d^2+h^2}}{c}\right) - \frac{1}{2\pi d} 0.5 I_{sc}\left(h, t - \frac{h}{c} - \frac{d}{c}\right) + \frac{1}{2\pi d} 0.5\rho_{gr} I_{sc}\left(h, t - \frac{h}{c} - \frac{d}{c}\right) \quad (15)$$

$$H_{\varphi\_flat}(d,t) = \frac{1}{2\pi d} I_{sc}\left(0, t - \frac{d}{c}\right) - \frac{1}{2\pi d}(1-\rho_{bot}) 0.5 I_{sc}\left(0, t - \frac{d}{c}\right) = \frac{1+\rho_{bot}}{2}\frac{1}{2\pi d} I_{sc}\left(0, t - \frac{d}{c}\right). \quad (16)$$

If ρ_{bot} = 1, equation (16) reduces to equation (11).

[36] Figures 9a and 9b show vertical electric field waveforms, calculated using equation (13) for a lightning strike to a 100-m-high object, on a perfectly conducting ground at horizontal distances of d = 30 and 300 m from the object, respectively. Figure 9c shows azimuthal magnetic field waveforms, calculated using equation (15) on a perfectly conducting ground at a horizontal distance of d = 30 m from the object. Azimuthal magnetic field waveforms at

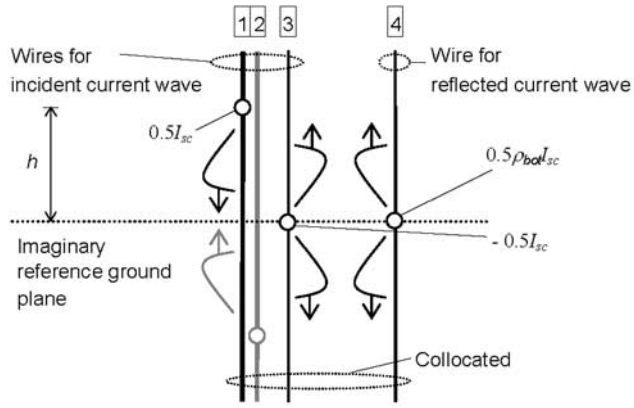

Figure 8. Approximation of the configuration shown in Figure 1a in the case of $\rho_{top} = 0$ ($Z_{ob} = Z_{ch}$) and $\rho_{bot} < 1$ ($Z_{gr} > 0$), comprising four collocated wires of vanishing radii and infinite longitudinal extent. Wires 1 and 2 are the same as the two wires shown in Figure 4b. They account for both incident current waves and current waves reflected perfectly from ground ($\rho_{bot} = 1$). Wires 3 and 4, energized at the reference ground plane, cancel the perfect ground reflection and add an imperfect ground reflection, respectively. Note that each wire supports unattenuated current waves propagating outward from the source and produces a spherical TEM wave.

d = 300 m are not shown in this paper, but their shapes are almost identical to those of vertical electric field waveforms at the same distance, shown in Figure 9b. In these calculations, we considered two values of ρ_{bot}, 0.7 and 1. The solid-line curves in Figure 9 are the total fields (total fields for $\rho_{bot} = 0$ are the same as the fields due to the incident current wave), dashed-line curves are the fields due to the incident current wave and dotted-line curves due to the reflected current wave.

[37] In Figure 9, the field waveforms due to incident current waves (dashed-line curves) begin to decay abruptly at time $t = (h + d)/c$: 0.43 μs for d = 30 m, and 1.3 μs for d = 300 m. At d = 30 m, the vertical electric field due to the incident current wave changes from about 4 kV/m to −5 kV/m, while the azimuthal magnetic field due to the same incident current wave decays from about 40 A/m to 30 A/m. At d = 300 m, the vertical electric field and azimuthal magnetic field (not shown here) due to the incident current wave exhibit similar waveshapes: They begin to decay abruptly after their peaks, at 1.3 μs, and then maintain their magnitudes at about 50% of the initial peak. This abrupt decay of incident fields is due to the second term, having the sign opposite to that of the first term, in equations (13) and (15), and signifies that the incident current wave is absorbed at the reference ground plane. In equation (13), the first term is a function of $1/\sqrt{(d^2 + h^2)}$, while the second (negative) term is a function of $1/d$. Therefore, at a very close horizontal distance, such as at d = 30 m, the magnitude of the second (negative) term becomes larger than that of the first term. This is the reason for the change of polarity of the vertical electric field due to the incident current wave at d = 30 m. In contrast, in equation (15), both the first term and the second (negative) term are each a function of $1/d$. Thus the azimuthal magnetic field due to the incident current wave remains unipolar.

[38] The information about conditions at ground (about current waves reflected from ground or about the absorption of the incident current wave at ground) arrives at the

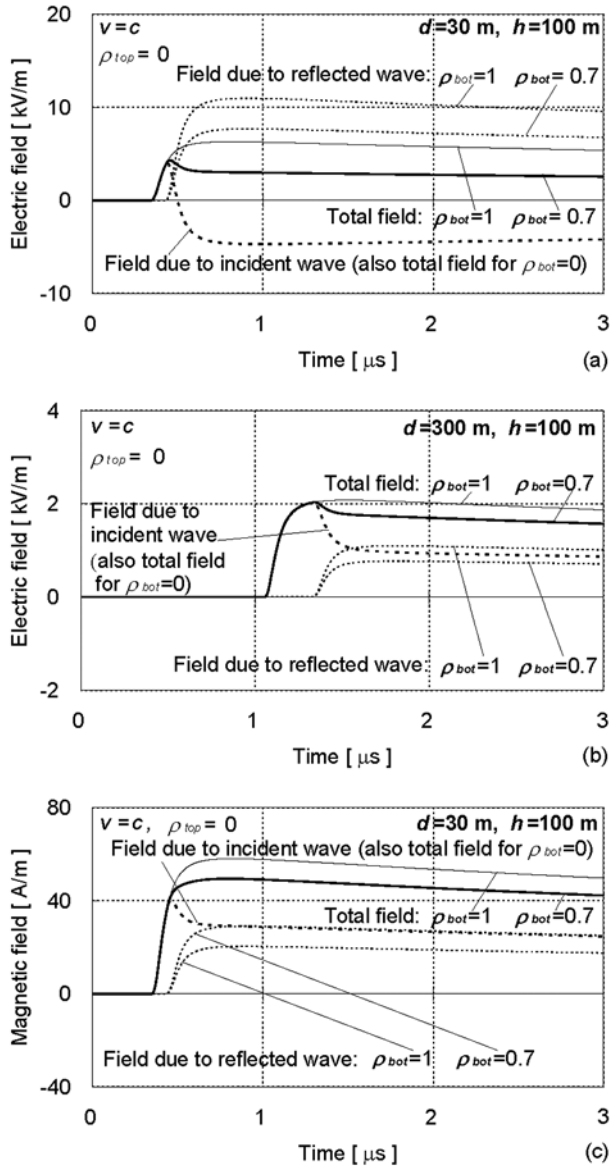

Figure 9. (a, b) Vertical electric field waveforms calculated using equation (13) for a lightning strike to a 100-m-high object on a perfectly conducting ground at horizontal distances of d = 30 m and d = 300 m from the object, respectively. (c) Azimuthal magnetic field waveforms calculated using equation (15) at a horizontal distance of d = 30 m from the object. Azimuthal magnetic field waveforms at d = 300 m, not shown in this paper, exhibit essentially the same shape as those of the vertical electric field waveforms shown in Figure 9b. The solid-line curves represent the total field (total field for $\rho_{bot} = 0$ is the same as the field due to the incident current wave), dashed-line curves represent the field due to the incident current wave and dotted-line curves due to the reflected current wave.

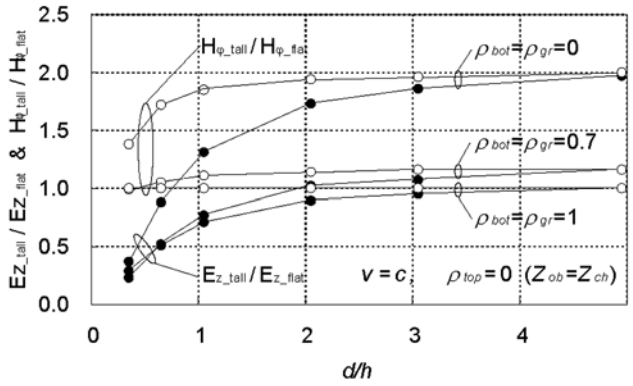

Figure 10. Illustration of the influence of imperfect current reflection from ground. Shown are ratios E_{z_tall}/E_{z_flat} (solid circles) and $H_{\varphi\_tall}/H_{\varphi\_flat}$ (open circles), each as a function of d/h, in the case of $v = c$, $\rho_{top} = 0$ ($Z_{ob} = Z_{ch}$) and $\rho_{bot} = \rho_{gr} = 1$, 0.7, and 0 ($Z_{gr} = 0$, 50, and 300 Ω if $Z_{ob} = Z_{ch} = 300$ Ω).

observation point $(h + d - \sqrt{(d^2 + h^2)})/c$ later than the information about the incident current wave injected at the top of the strike object. For example, this time delay is about 0.1 μs if $d = 30$ m and $h = 100$ m, and about 0.3 μs if $d = 300$ m and $h = 100$ m. As a consequence, the influence of ground reflection is smaller for more distant observation points and taller strike objects. Also, the first term in equation (13) varies approximately as $1/d$ if $d \gg h$. Thus the distance dependence of the vertical electric field is similar to that of the azimuthal magnetic field at a distant observation point.

[39] We now discuss distance dependences of the ratio of fields due to a lightning strike to a tall object and those due to the same strike to flat ground, in the case of $v = c$, $\rho_{top} = 0$ (corresponding to $Z_{ob} = Z_{ch}$), and three values of $\rho_{bot} = 1$, 0.7, and 0 (corresponding to $Z_{gr} = 0$, 50, and 300 Ω, respectively, if $Z_{ob} = Z_{ch} = 300$ Ω). For $\rho_{gr} = 0.7$, the magnitude of current waves injected initially into the channel and into the object from the source in the configuration shown in Figure 1a (strike to tall object) is $(1 - \rho_{top})I_{sc}(h, t)/2 = 0.5I_{sc}(h, t)$, and that of the current wave injected into the channel from the source in the configuration shown in Figure 1b (strike to flat ground) is $(1 + \rho_{gr})I_{sc}(0, t)/2 = 0.85I_{sc}(0, t)$.

[40] The computed ratios E_{z_tall}/E_{z_flat} and $H_{\varphi\_tall}/H_{\varphi\_flat}$, each as a function of d/h, are shown in Figure 10. It is clear from Figure 10 that the ratios E_{z_tall}/E_{z_flat} and $H_{\varphi\_tall}/H_{\varphi\_flat}$ increase with decreasing ρ_{bot}. The former ratio exceeds unity when d/h is about 0.7 and 2 for $\rho_{bot} = \rho_{gr} = 0$ and 0.7, respectively. As d/h increases, both the electric and magnetic field ratios approach the far field enhancement factor given by $(1 - \rho_{top})(c/v + 1)/(1 + \rho_{gr})$ (see equation (B5) in Appendix B), which is equal to 2 for $\rho_{top} = 0$, $\rho_{gr} = 0$, and $v = c$, and 1.17 for $\rho_{top} = 0$, $\rho_{gr} = 0.7$, and $v = c$.

5. Influence of Current Reflection at the Top of the Tall Strike Object

[41] Here, we examine the influence of the assumption $\rho_{top} = 0$ made in the basic case (see section 3), assuming $\rho_{top} = -0.5$ in section 5.1 and considering three values of ρ_{top}, 0, −0.5, and −1, in section 5.2.

5.1. Comparison of a Lightning Strike to a Tall Object With That to Flat Ground

[42] In this section we assume that $\rho_{top} = -0.5$ (corresponding, for example, to $Z_{ob} = 300$ Ω and $Z_{ch} = 900$ Ω), with all other conditions being the same as in the basic case, presented in section 3. Note that *Janischewskyj et al.* [1996], from their analysis of five current waveforms measured 474 m above ground on the CN tower, inferred ρ_{top} to vary from −0.27 to −0.49, and *Fuchs* [1998], from 13 simultaneous current measurements at the top and bottom of the Peissenberg tower, found ρ_{top} to vary from −0.39 to −0.68.

[43] Figures 11 and 12, to be compared with Figures 2a and 3a, show waveforms of vertical electric field and azimuthal magnetic field, respectively. The corresponding field waveforms calculated for the same lightning strike to flat ground are the same as those shown in Figures 2b and 3b, respectively. The fields were calculated in the same manner as in section 3.1. Note that the magnitude of current waves injected into the channel and into the object from the source at the top of the object (see Figure 1a) is $(1 - \rho_{top})I_{sc}(h, t)/2 = 0.75I_{sc}(h, t)$ and that of current wave injected into the channel from the source at ground level (see Figure 1b) is $(1 + \rho_{gr})I_{sc}(0, t)/2 = I_{sc}(0, t)$.

[44] As seen in Figures 11 and 12, the influence of current waves reflected from the top of the 100-m-high object first appears in the field waveforms at $t = 2h/c + \sqrt{(d^2 + h^2)}/c$: for example, at 1.0 μs at $d = 30$ m and at 1.7 μs at $d = 300$ m. At each distance, the field reaches its peak before the information about current waves reflected from the object top arrives at the observation point. If the strike object is higher than 100 m, this information arrives at the observation point even later. Thus the current "reflection" itself at the top of 100-m-high object does not influence the peak values of electric and magnetic fields. However, since the magnitude of current waves injected into the channel and into the object from the source, which is given by $(1 - \rho_{top})I_{sc}(h, t)/2$, increases with decreasing

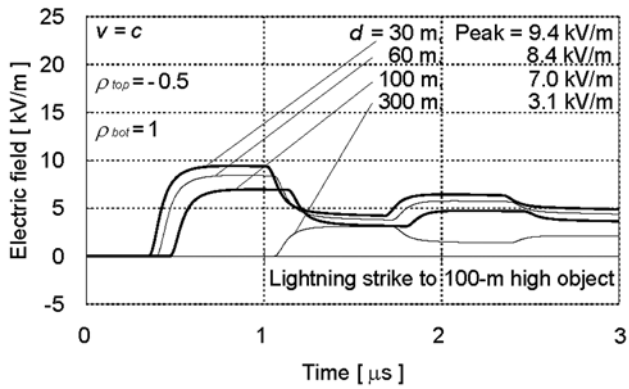

Figure 11. Reflection from the object top case ($\rho_{bot} = \rho_{gr} = 1$, $\rho_{top} = -0.5$, $v = c$). Vertical electric field waveforms due to a lightning strike to 100-m-high object at horizontal distances of $d = 30$, 60, 100, and 300 m from the lightning channel.

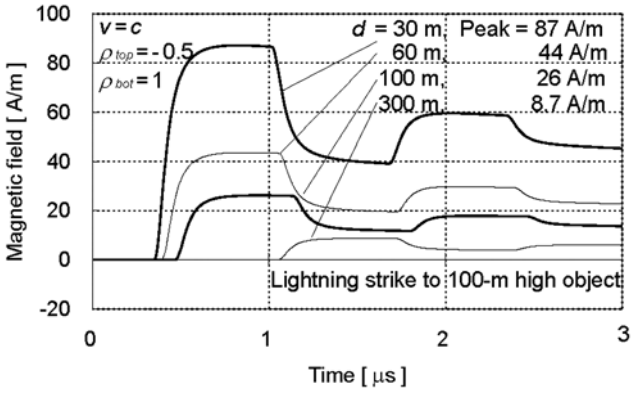

Figure 12. Same as Figure 11, but for the azimuthal magnetic field. Azimuthal magnetic field waveforms due to the same lightning to flat ground are the same as those shown in Figure 3b.

ρ_{top} ($\rho_{top} < 0$), the field magnitudes increase with decreasing ρ_{top}. Note that in the case of $\rho_{bot} = 0$ ($Z_{ob} = Z_{gr}$), ρ_{gr} becomes equal to $-\rho_{top}$ (see equations (1) and (4)), and thereby $(1 - \rho_{top})I_{sc}/2$ becomes equal to $(1 + \rho_{gr})I_{sc}/2$, regardless of the value of ρ_{top}. In this special case ($\rho_{bot} = 0$), the ratios of E_{z_tall}/E_{z_flat} and $H_{\varphi\_tall}/H_{\varphi\_flat}$ are independent of the value of ρ_{top}.

[45] In the case of $\rho_{top} = -0.5$, the peak of the vertical electric field due to a lightning strike to the 100-m-high object is smaller than that due to the same strike to flat ground at d = 30 and 60 m, but is larger at d = 100 and 300 m (compare Figures 11 and 2b). This indicates that the presence of strike object with $\rho_{top} < 0$ serves to attenuate relatively close electric fields and enhance relatively distant electric fields.

[46] The peak of the azimuthal magnetic field due to a lightning strike to the 100-m-high object in the case of $\rho_{top} = -0.5$ is 1.5 times larger than that due to the same strike to flat ground at any horizontal distance (compare Figures 12 and 3b). Recall that when $\rho_{top} = 0$, the former is identical to the latter. This indicates that the presence of strike object with $\rho_{top} < 0$ serves to enhance magnetic fields.

5.2. Analysis of Distance Dependences of the Ratios of Electric and Magnetic Fields for Tall-Object and Flat-Ground Cases

[47] The ratios E_{z_tall}/E_{z_flat} and $H_{\varphi\_tall}/H_{\varphi\_flat}$, each as a function of d/h, in the case of $\rho_{bot} = \rho_{gr} = 1$ (corresponding to $Z_{gr} = 0$) and $\rho_{top} = 0$, -0.5, and -1 (corresponding to $Z_{ch} = Z_{ob}$, $Z_{ch} = 3Z_{ob}$, and $Z_{ch} \gg Z_{ob}$) are shown in Figure 13. The magnitudes of current waves injected into the channel and into the object from the source at the top of the object (see Figure 1a), given by $(1 - \rho_{top})I_{sc}(h, t)/2$, are $0.5I_{sc}(h, t)$, $0.75I_{sc}(h, t)$, and $I_{sc}(h, t)$ for $\rho_{top} = 0$, -0.5, and -1, respectively. The magnitude of current wave injected into the channel from the source at ground level (see Figure 1b), given by $(1 + \rho_{gr})I_{sc}(0, t)/2$, is $I_{sc}(0, t)$.

[48] It is clear from Figure 13 that the ratios E_{z_tall}/E_{z_flat} and $H_{\varphi\_tall}/H_{\varphi\_flat}$ increase with decreasing ρ_{top}. The former exceeds 1 when d/h is about 1 and 0.6 for $\rho_{top} = -0.5$ and -1, respectively. At larger distances, the electric field ratio approaches 1, 1.5, and 2 for $\rho_{top} = 0$, -0.5, and -1, respectively. The magnetic field ratio is independent of d/h and equal to 1, 1.5, and 2 for $\rho_{top} = 0$, -0.5, and -1, respectively. The distant electric field ratios and magnetic field ratios are equal to the far field enhancement factor given by $(1 - \rho_{top})(c/v + 1)/(1 + \rho_{gr})$ (see equation (B5) in Appendix B).

6. Influence of Return-Stroke Speed Being Less Than the Speed of Light

[49] Here we examine the influence of the assumption $v = c$ made in the basic case (see section 3), considering two values of return-stroke speed, $v = c$ and $v = 0.5c$.

6.1. Comparison of a Lightning Strike to a Tall Object With That to Flat Ground

[50] In this section, we assume that $v = 0.5c$, with all other conditions being the same as in the basic case, presented in section 3. Note that typical values of return stroke wave front speed are one third to two thirds of c [e.g., *Rakov*, 2004]. Also note that since any current wave is assumed to propagate along the lightning channel at speed v (see equation (2b)), ground-reflected current waves are unable to catch up with the return-stroke front, and hence there is no need to deal with reflections at the front.

[51] Figure 14a (to be compared with Figure 2a) shows vertical electric field waveforms for a lightning strike to the 100-m-high object, and Figure 14b (to be compared with Figure 2b) shows the corresponding electric field waveforms for the same lightning strike to flat ground. Figures 15a and 15b are the same as Figures 14a and 14b, respectively, but for azimuthal magnetic fields. The fields were calculated in the same manner as in section 3.1. Note that vertical scales in Figures 14a and 14b are different, while in Figures 15a and 15b they are the same.

[52] As seen in Figures 14a and 14b, in the case of $v = 0.5c$, the peak of the vertical electric field due to a lightning strike to the 100-m-high object is smaller than that due to the same strike to flat ground for all distances considered (d = 30 to 300 m). The vertical electric fields within d = 300 m reach their peaks, which are shown in the upper

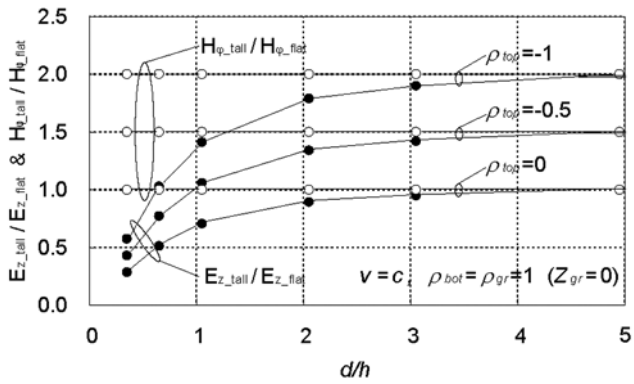

Figure 13. Illustration of the influence of current reflection at the top of the tall strike object. Shown are ratios E_{z_tall}/E_{z_flat} (solid circles) and $H_{\varphi\_tall}/H_{\varphi\_flat}$ (open circles), each as a function of d/h, in the case of $v = c$, $\rho_{bot} = \rho_{gr} = 1$ ($Z_{gr} = 0$) and $\rho_{top} = 0$, -0.5, and -1 ($Z_{ch} = Z_{ob}$, $Z_{ch} = 3Z_{ob}$, and $Z_{ch} \gg Z_{ob}$).

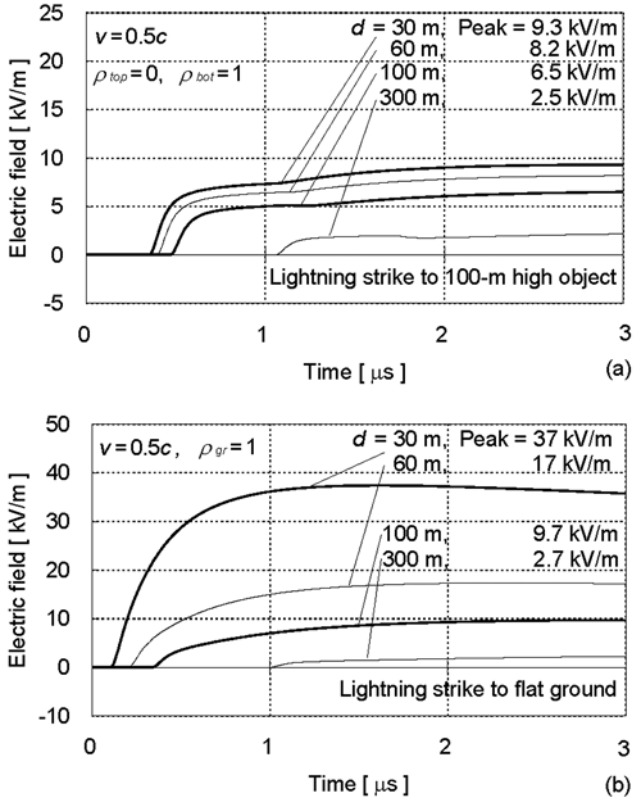

Figure 14. Less than the speed of light case ($\rho_{bot} = \rho_{gr} = 1$, $\rho_{top} = 0$ $v = 0.5c$). Vertical electric field waveforms (a) due to a lightning strike to 100-m-high object and (b) due to the same lightning strike to flat ground, at horizontal distances of d = 30, 60, 100, and 300 m from the lightning channel.

right corner of Figures 14a and 14b, within 7 μs, although the field waveforms are shown only up to 3 μs.

[53] As seen in Figures 15a and 15b, the peak of the azimuthal magnetic field due to a lightning strike to the 100-m-high object is larger than that due to the same strike to flat ground for all distances considered (d = 30 to 300 m). This is in contrast with the case of $v = c$ (see Figures 3a and 3b) for which the magnetic fields are independent of the presence of the strike object. The azimuthal magnetic field peaks are shown in the upper right corner of Figures 15a and 15b. At d = 300 m, the peak occurs at about 4 μs in Figure 15b, although the field waveforms are shown only up to 3 μs.

6.2. Analysis of Distance Dependences of the Ratios of Electric and Magnetic Fields for Tall-Object and Flat-Ground Cases

[54] The ratios E_{z_tall}/E_{z_flat} and $H_{\varphi\_tall}/H_{\varphi\_flat}$, each as a function of d/h, in the case of $\rho_{bot} = \rho_{gr} = 1$, $\rho_{top} = 0$, and $v = 0.5c$ and c, are shown in Figures 16a and 16b. The magnitude of current waves injected into the channel and into the object from the source at the top of the strike object (see Figure 1a) is $0.5I_{sc}(h, t)$, and that of current wave injected into the channel from the source at ground level (see Figure 1b) is $I_{sc}(0, t)$.

[55] It is clear from Figure 16a that in the vicinity of strike object ($d < 3h$), the ratios E_{z_tall}/E_{z_flat} and $H_{\varphi\_tall}/H_{\varphi\_flat}$ for $v = 0.5c$ are almost the same as those for $v = c$. The abrupt increase in the ratio E_{z_tall}/E_{z_flat} between $d = 20h$ and $30h$ (see Figure 16b) is due to the fact that for $d \leq 20h$ both E_{z_tall} and E_{z_flat} rise to their peaks in several microseconds or more while for $d > 30h$ the fields rise to their peaks within 1 μs (because the radiation field component becomes dominant at larger distances). Beyond $d = 30h$, ratios E_{z_tall}/E_{z_flat} and $H_{\varphi\_tall}/H_{\varphi\_flat}$ attain the value of 1.5, which is equal to the far field enhancement factor given by $(1 - \rho_{top})(c/v + 1)/(1 + \rho_{gr}) = 1.5$ (see equation (B5) in Appendix B).

[56] In the following, we will estimate the influence of strike object height (see Figure 17) and return-stroke current risetime (see Figure 18). As seen in Figure 17, the overall variation of the ratio E_{z_tall}/E_{z_flat} for the case h = 200 m is quite similar to that for h = 100 m (see Figure 16). When a current waveform whose risetime is 3 times longer than that of the current waveform proposed by *Nucci et al.* [1990] is used, the ratio E_{z_tall}/E_{z_flat} increases abruptly between $d = 30h$ and $40h$, as seen in Figure 18b and in contrast with Figure 16b. The modified, longer current risetime is longer than $h/c = 0.33$ μs. As a result, the ratios E_{z_tall}/E_{z_flat} and $H_{\varphi\_tall}/H_{\varphi\_flat}$ assymptotically approach 1.34, which is smaller than the far field enhancement factor given by $(1 - \rho_{top})(c/v + 1)/(1 + \rho_{gr}) = 1.5$.

[57] It appears from Figure 16 that at shorter distances, $d < h$, equations (8) and (12) derived assuming $\rho_{bot} = \rho_{gr} = 1$, $\rho_{top} = 0$, and $v = c$ also reasonably represent the case of $\rho_{bot} = \rho_{gr} = 1$, $\rho_{top} = 0$, and $v = 0.5c$. On the other hand, since the ratios are dependent on the values of ρ_{bot},

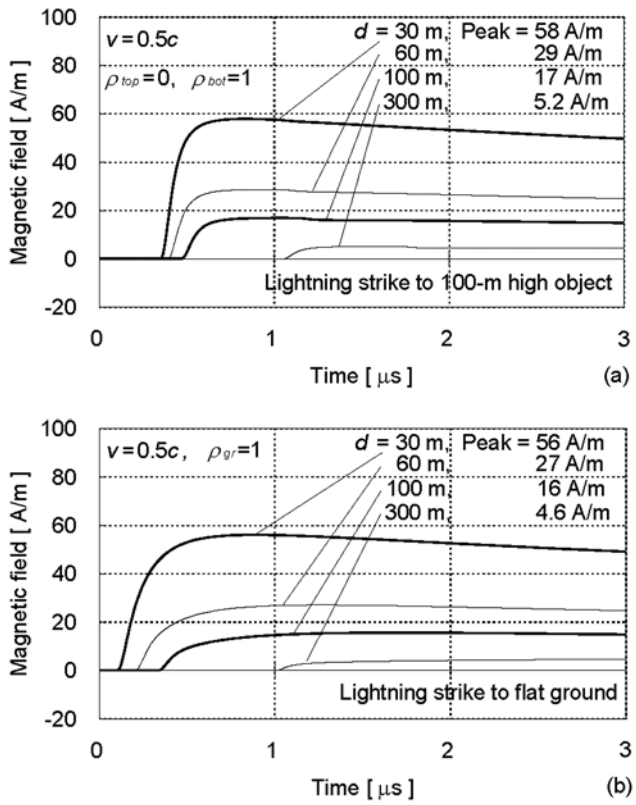

Figure 15. Same as Figure 14, but for the azimuthal magnetic field.

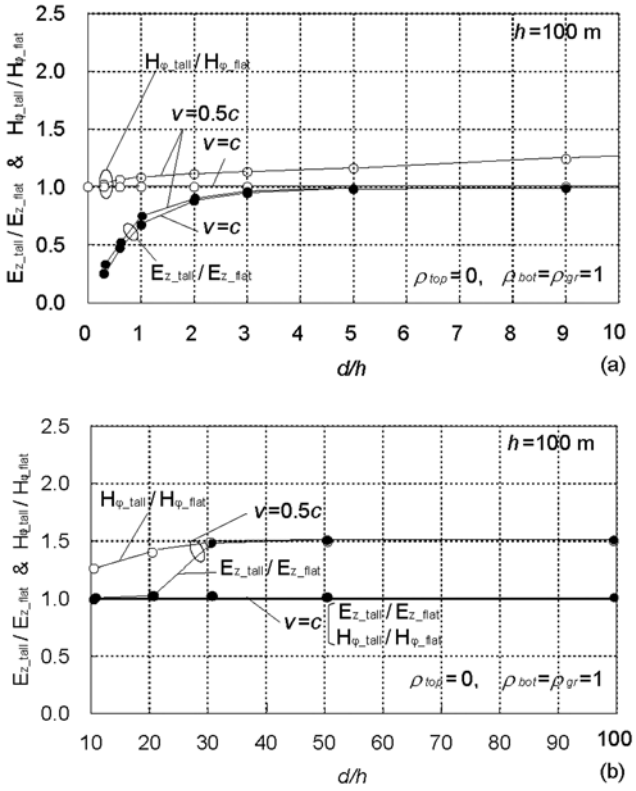

Figure 16. Illustration of the influence of return-stroke speed being less than the speed of light for (a) $d/h < 10$, and (b) $10 \leq d/h \leq 100$. Shown are ratios E_{z_tall}/E_{z_flat} (solid circles) and $H_{\varphi\_tall}/H_{\varphi\_flat}$ (hollow circles), each as a function of d/h, in the case of $\rho_{bot} = \rho_{gr} = 1$ ($Z_{gr} = 0$), $\rho_{top} = 0$ ($Z_{ch} = Z_{ob}$), and $v = 0.5c$ and c.

ρ_{gr}, and ρ_{top} (as is clear from Figures 10 and 13), these equations are not necessarily valid for arbitrarily specified values of ρ_{bot}, ρ_{gr}, and ρ_{top}.

7. Comparison With Experimental Data

[58] As noted in section 1, *Fisher and Schnetzer* [1994] experimentally found that a strike object appeared to reduce electric fields in its vicinity. They examined the dependence of triggered lightning electric fields on the height of a strike object at Fort McClellan, Alabama. The fields were measured at distances of $d = 9.3$ and 19.3 m from a vertical grounded metallic rod whose height h was either 4.5 or 11 m. They observed that the leader electric fields (approximately equal to return stroke fields at these distances) tend to be reduced as the strike object height increases. Ratios of the average vertical electric field on ground due to lightning strikes to the 11-m-high object to that due to strikes to the 4.5-m-high object at $d = 9.3$ m and 19.3 m, based on the experimental data of *Fisher and Schnetzer* [1994], are given in Table 2. Note that the sample sizes for the 11-m-high and 4.5-m-high objects are 3 and 8, respectively, and the measured vertical electric fields are normalized by the corresponding measured return-stroke peak currents.

[59] We computed the corresponding ratios, using the models described in sections 2–6, for three sets of parameters, (1) $\rho_{top} = 0$, $\rho_{bot} = 1$, $v = c$ (see section 3), (2) $\rho_{top} = -0.5$, $\rho_{bot} = 1$, $v = c$ (see section 5), and (3) $\rho_{top} = -0.5$, $\rho_{bot} = 1$, $v = 0.5c$ (a physically reasonable case). The results are also presented in Table 2. In all cases considered, model-predicted electric field ratios are in fair agreement with the experimental data of *Fisher and Schnetzer* [1994]. A smaller ratio at a closer distance indicates a more significant shielding effect for smaller values of d/h. It is worth noting that 4.5-m and 11-m strike objects act as transmission lines only at frequencies higher than about 3 MHz (wavelengths shorter than 100 m); at lower frequencies, they act as lumped circuits, since the wavelengths are much larger than the strike-object height.

8. Comparison With Other Modeling Studies

[60] As noted in section 1, *Rachidi et al.* [2001] showed that E_{z_tall} and H_{φ_tall} at $d = 2$ km from a tower of height $h = 553$ m struck by lightning were 2.6 times larger than E_{z_flat} and H_{φ_flat}. They assumed that $v = 0.63c$, $\rho_{top} = -0.5$, and $\rho_{bot} = 0.48$ (corresponding, for example, to $Z_{ch} = 900\ \Omega$, $Z_{ob} = 300\ \Omega$, and $Z_{gr} = 100\ \Omega$, in which case $\rho_{gr} = 0.8$). They injected the same current from their model source into the tower and into the lightning channel in the case of strike to the tower as that injected into the channel at $z' = 0$ in the case of strike to flat ground. In order to assure the same charge transfer to ground (see section 2), according to equations (2a), (2b), and (3), the injected currents should be $(1 - \rho_{top})I_{sc}/2 = 0.75I_{sc}$ and $(1 + \rho_{gr})I_{sc}/2 = 0.9I_{sc}$ for the tall-object and flat-ground cases, respectively. Thus, Rachidi

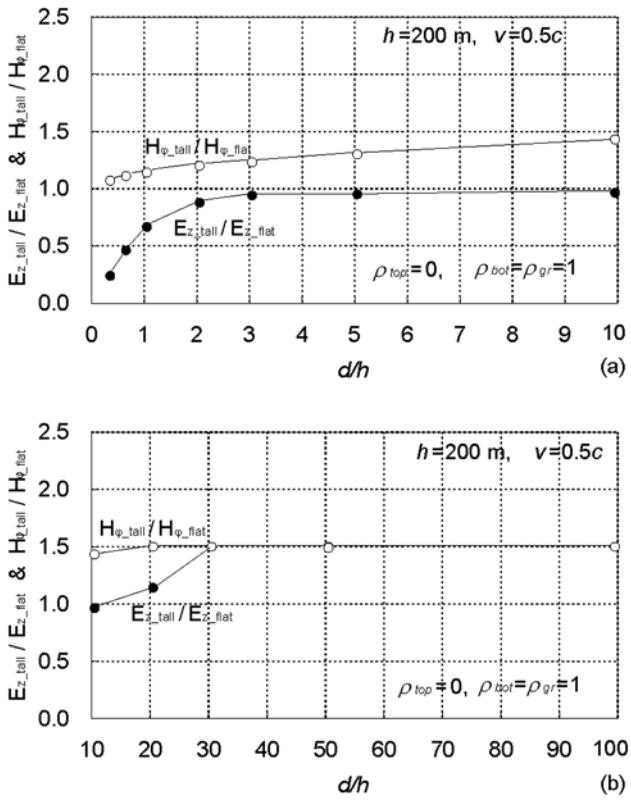

Figure 17. Same as Figure 16, but for $h = 200$ m and $v = 0.5c$ only.

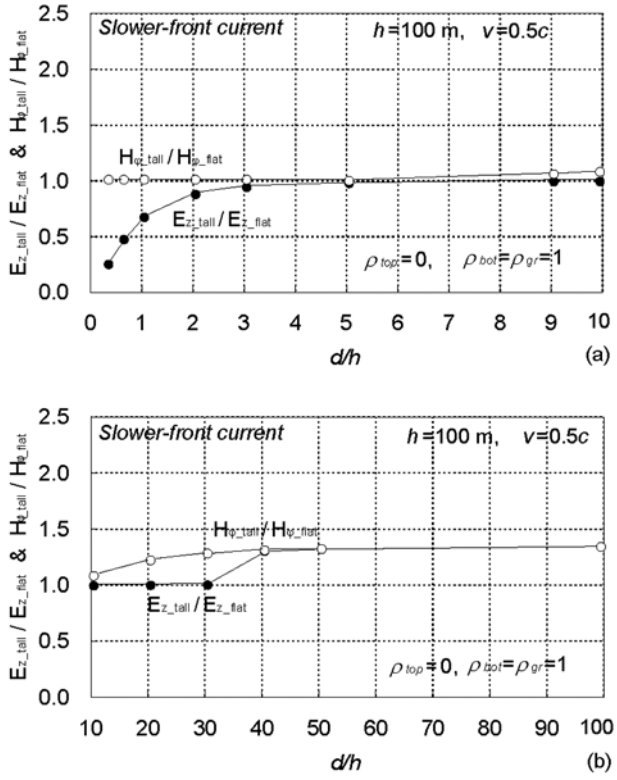

Figure 18. Same as Figure 16, but for a slower-rising current waveform, whose risetime is 3 times longer than that of the current waveform, thought to be typical for lightning subsequent return strokes proposed by *Nucci et al.* [1990].

et al.'s ratios E_{z_tall}/E_{z_flat} and $H_{\varphi\_tall}/H_{\varphi\_flat}$, adjusted to normalize them to the same charge transfer to ground, should be equal to 2.2 (=2.6 × 0.75/0.9). Although *Rachidi et al.* [2001] used the MTLE model to represent the lightning channel, this adjusted ratio is in good agreement with the far field enhancement factor derived in this paper using the TL model, which is given by $(1 - \rho_{top})(c/v + 1)/(1 + \rho_{gr})$ (see equation (B5) of Appendix B and Table 3).

[61] As discussed in section 1, *Miyazaki and Ishii* [2004] showed, based on their calculations using an electromagnetic model (NEC-2), that for h = 60 to 240 m the ratio E_{z_tall}/E_{z_flat} was smaller than 1 at d = 100 to 600 m and larger than 1 beyond d = 600 m, while the ratio $H_{\varphi\_tall}/H_{\varphi\_flat}$, was larger than 1 beyond d = 100 m. These ratios reached their peaks (about 1.9 when a current wave having a zero-to-peak risetime of about 1 μs was injected, while the zero-to-peak risetime of the current wave we use in this paper is about 0.4 μs) around several kilometers from the channel, and then began to decrease with increasing horizontal distance. In their calculations, the lightning channel was represented by a vertical wire having 1-Ω/m distributed resistance and 3-μH/m additional distributed inductance. The current waves propagated at about $v = 0.5c$ with attenuation and dispersion along this channel. The characteristic impedance of the channel is estimated by us to be about 700 Ω. Miyazaki and Ishii injected current waves into the channel and into the tall object (represented by a vertical perfectly conducting wire whose characteristic impedance Z_{ob} was about 200 Ω) from a voltage source having internal resistance of 300 Ω (thus the equivalent impedance of the lightning channel should be Z_{ch} = 700 + 300 = 1 kΩ). They set the ground conductivity to 0.003 S/m, and inserted the lumped resistance between the strike object and the 0.003-S/m ground. The total grounding impedance, which was the sum of the inserted lumped resistance and the grounding impedance due to the 0.003-S/m ground, is not given. No lumped grounding resistance was used in simulating strikes to flat ground. Thus the total charge transfer to ground for the flat-ground case is probably slightly different from that for the strike-object case. On the basis of the above, $v = 0.5c$, $\rho_{top} = -0.67$, $\rho_{bot} = 0.74$, and $\rho_{gr} = 1$ (ρ_{bot} and ρ_{gr} do not account for the 0.003-S/m ground), although these parameters vary depending on frequency in their model. The far-field enhancement factor calculated using these parameters and equation (B5) is given in Table 3. Note that even if we consider the grounding impedance due to the 0.003-S/m ground as 30-Ω resistance ($\rho_{gr} = 0.94$), for example, the far field enhancement factor will only increase by 3% relative to its value given in Table 3.

9. Summary

[62] We examined the electric field and magnetic field ratios for the cases of strikes to the tall object and to flat ground as a function of distance from the lightning channel, current reflection coefficients at ground and at the top of the strike object, and return-stroke speed, v. The total charge transfer to ground was the same regardless of the presence of strike object. In close proximity to the strike object, the vertical electric field is reduced relative to the flat-ground case, while the azimuthal magnetic field is either enhanced or independent of the presence of strike object. At far distances, both the electric and magnetic fields due to strikes to the tall object are enhanced relative to the flat-ground case. For example, if $\rho_{top} = -0.5$, $\rho_{gr} = 1$, and $v = 0.5c$, where ρ_{top} is the current reflection coefficient at the top of the object for upward-propagating waves and ρ_{gr} is that at the lightning channel base when the channel terminates directly on ground, the field enhancement factor is equal to 2.3.

[63] The above findings regarding the lightning electromagnetic environment in the presence of a tall strike object have important implications for studying lightning return-stroke processes at early times and for optimizing lightning

Table 2. Ratios of Vertical Electric Field on Ground Due to Strikes to the 11-m-High Object to That Due to Strikes to the 4.5-m-High Object at 9.3 and 19.3 m Reported by *Fisher and Schnetzer* [1994] Versus Those Predicted by Models Described in This Paper

	Distance From Lightning Channel	
Model Parameters	9.3 m	19.3 m
$\rho_{top} = 0$, $\rho_{bot} = 1$, and $v = c$	0.72	0.89
$\rho_{top} = -0.5$, $\rho_{bot} = 1$, and $v = c$	0.72	0.90
$\rho_{top} = -0.5$, $\rho_{bot} = 1$, and $v = 0.5c$	0.70	0.88
Experiment [*Fisher and Schnetzer*, 1994]	0.45	0.65

Table 3. Comparison of Ratios E_{z_tall}/E_{z_flat} and $H_{\varphi\_tall}/H_{\varphi\_flat}$ at d = 2 km Predicted by Different Models

Model	E_{z_tall}/E_{z_flat} or $H_{\varphi\_tall}/H_{\varphi\_flat}$	Parameters
Rachidi et al. [2001] (MTLE)	2.6 (2.2)[a]	$\rho_{top} = -0.50$, $\rho_{bot} = 0.48$, $\rho_{gr} = 0.8$, $v = 0.63c$
This paper (equation (B5))	2.2	$\rho_{top} = -0.50$, $\rho_{bot} = 0.48$, $\rho_{gr} = 0.8$, $v = 0.63c$
Miyazaki and Ishii [2004] (NEC-2)	1.9	$\rho_{top} = -0.67$, $\rho_{bot} = 0.74$, $\rho_{gr} = 1.0$, $v = 0.5c$
This paper (equation (B5))	2.5	$\rho_{top} = -0.67$, $\rho_{bot} = 0.74$, $\rho_{gr} = 1.0$, $v = 0.5c$

[a]The ratio given in the parentheses was obtained by adjusting *Rachidi et al.*'s [2001] value, 2.6, to normalize it to the same charge transfer to ground for the tall-object and flat-ground cases.

protection means of nearby telecommunication and power distribution lines.

Appendix A: Total Charge Transfer to Ground in the Case of Lightning Strike to Flat Ground Versus That to Tall Object

[64] We show in this appendix that the total charge transfer to ground in our representation of lightning is independent of the presence of strike object, as required for comparison of the tall-object and flat-ground cases. The total charge transferred to ground in the case of lightning strike to flat ground is found by integrating current given by equation (3) at $z' = 0$

$$Q_{flat} = \int_0^\infty I(0,t)dt = \frac{1+\rho_{gr}}{2}\int_0^\infty I_{sc}(0,t)dt = \frac{Z_{ch}}{Z_{ch}+Z_{gr}}\int_0^\infty I_{sc}(0,t)dt. \quad \text{(A1)}$$

The total charge transferred to ground in the case of lightning strike to a tall grounded object is found by integrating current given by equation (2a) at $z' = 0$

$$\begin{aligned} Q_{tall} &= \int_0^\infty I(0,t)dt \\ &= \frac{1-\rho_{top}}{2}\int_0^\infty \sum_{n=0}^{\infty}\left[\begin{array}{l}\rho_{bot}^n\rho_{top}^n I_{sc}\left(h,t-\frac{h}{c}-\frac{2nh}{c}\right)\\ +\rho_{bot}^{n+1}\rho_{top}^n I_{sc}\left(h,t-\frac{h}{c}-\frac{2nh}{c}\right)\end{array}\right]dt \\ &= \frac{1-\rho_{top}}{2}(1+\rho_{bot})\int_0^\infty \sum_{n=0}^{\infty}\rho_{bot}^n\rho_{top}^n I_{sc}\left(h,t-\frac{h}{c}-\frac{2nh}{c}\right)dt \\ &= \frac{1-\rho_{top}}{2}(1+\rho_{bot})\int_0^\infty \cdot\left[\begin{array}{l}\sum_{n=0}^{m}\rho_{bot}^n\rho_{top}^n I_{sc}\left(h,t-\frac{h}{c}-\frac{2nh}{c}\right)\\ +\sum_{n=m+1}^{\infty}\rho_{bot}^n\rho_{top}^n I_{sc}\left(h,t-\frac{h}{c}-\frac{2nh}{c}\right)\end{array}\right]dt, \end{aligned} \quad \text{(A2)}$$

where n is an index representing the successive multiple reflections occurring at the two ends of the strike object, and m is the maximum value of n satisfying the condition that $t - h/c - 2nh/c$ (see the argument of I_{sc} in equation (A2)) is larger than the duration, T_d, of $I_{sc}(h, t)$ when t approaches infinity. Note that $I_{sc}(h, t) = 0$ when $t < 0$ and $t > T_d$. Thus, m becomes equal to infinity ($n < c(t - T_d)/2 - 0.5$) at $t \to \infty$ when T_d is finite. When this latter condition of finite $I_{sc}(h, t)$ duration is satisfied,

$$\int_0^\infty I_{sc}\left(h,t-\frac{h}{c}-\frac{2nh}{c}\right)dt = \int_0^\infty I_{sc}(h,t)dt \qquad 0 \le n \le m$$
$$\left|\int_0^\infty I_{sc}\left(h,t-\frac{h}{c}-\frac{2nh}{c}\right)dt\right| < \int_0^\infty I_{sc}(h,t)dt \qquad n > m \quad \text{(A3)}$$

$$\rho_{bot}^n\rho_{top}^n \approx 0 \qquad \text{for } \left|\rho_{bot}\rho_{top}\right| < 1 \text{ and } n \ge m. \quad \text{(A4)}$$

Using equations (A3) and (A4), equation (A2) can be written as

$$\begin{aligned} Q_{tall} &\cong \frac{1-\rho_{top}}{2}(1+\rho_{bot})\left[\sum_{n=0}^{m}\rho_{bot}^n\rho_{top}^n\int_0^\infty I_{sc}(h,t)dt + 0\right] \\ &\cong \frac{1-\rho_{top}}{2}(1+\rho_{bot})\frac{1}{1-\rho_{bot}\rho_{top}}\int_0^\infty I_{sc}(h,t)dt \\ &= \frac{Z_{ch}}{Z_{ch}+Z_{gr}}\int_0^\infty I_{sc}(h,t)dt. \end{aligned} \quad \text{(A5)}$$

Since the infinite time integral of lightning short-circuit current in equation (A5) is the same as that in equation (A1), the total charge transferred to ground is the same in both cases, $Q_{tall} = Q_{flat}$. Note that the geometrical series in equation (A5) is reduced as $\sum_{n=0}^{m}\rho_{bot}^n\rho_{top}^n = 1/(1 - \rho_{bot}\rho_{top})$ [e.g., *Spiegel and Liu*, 1998] since $|\rho_{bot}\rho_{top}|$ is less than 1 (unless $Z_{ch} = 0$ or ∞, which is physically unreasonable). We conclude that lightning represented by current Equations (2a) and (2b) for the tall-object case is the same as that represented by current equation (3) for the flat-ground case.

Appendix B: Far Field Enhancement Factor Due to the Presence of Tall Strike Object

B1. Far Field Enhancement Factor Based on the Model Presented in This Paper

[65] In this appendix we derive an equation for the far field (either electric or magnetic) enhancement factor due to the presence of tall strike object, using current Equations (2a), (2b), and (3). The far field enhancement factor is defined here as the ratio of electric or magnetic radiation field peaks for the strike-object and flat-ground cases.

[66] The far (essentially radiation) electric field on perfectly conducting ground plane due to a current wave propagating along an infinitely long vertical channel

attached to an object of height h is given by [*Uman et al.*, 1975]

$$E^{far}_{z\_cha}\left(d, t+\frac{d}{c}\right) \cong -\frac{1}{2\pi\varepsilon_0 c^2 d}\, v\, I(h,t). \tag{B1a}$$

Similarly, the far electric field on perfectly conducting ground plane due to a current wave propagating along the tall object, which is produced (injected or reflected) at the top of the object, and that due to a current wave, which is produced (reflected) at the bottom of the object, are given, respectively, by

$$E^{far}_{z\_top}\left(d, t+\frac{d}{c}\right) \cong -\frac{1}{2\pi\varepsilon_0 c^2 d}\, c\, \left[I(h,t) - I\left(h, t-\frac{h}{c}\right)\right] \tag{B1b}$$

$$E^{far}_{z\_bot}\left(d, t+\frac{d}{c}\right) \cong -\frac{1}{2\pi\varepsilon_0 c^2 d}\, c\, \left[I(0,t) - I\left(0, t-\frac{h}{c}\right)\right]. \tag{B1c}$$

Note that the second term in equations (B1b) and (B1c) represents the so-called mirror image effect [*Uman et al.*, 1975]. The total far vertical electric field due to a lightning strike to an object of height h is given by

$$E^{far}_{z\_tall}\left(d, t+\frac{d}{c}\right) = E^{far}_{z\_cha}\left(d, t+\frac{d}{c}\right) + E^{far}_{z\_top}\left(d, t+\frac{d}{c}\right) + E^{far}_{z\_bot}\left(d, t+\frac{d}{c}\right). \tag{B2a}$$

Substituting equation (2b) in equation (B1a) and equation (2a) in equations (B1b) (the first term) and (B1c) (the second term), and then (B1a), (B1b), and (B1c) in (B2a), one can obtain

$$E^{far}_{z\_tall}\left(d, t+\frac{d}{c}\right) = -\frac{1}{2\pi\varepsilon_0 c^2 d}\frac{\left(1-\rho_{top}\right)(c+v)}{2} I_{sc}(h,t) - \frac{1}{2\pi\varepsilon_0 c^2 d}\frac{1-\rho_{top}}{2}\sum_{n=0}^{\infty} \cdot \begin{bmatrix} v\rho_{bot}^{n+1}\rho_{top}^{n}\left(1+\rho_{top}\right) I_{sc}\left(h, t-\frac{2(n+1)h}{c}\right) \\ +c\left(\rho_{top}-1\right)\rho_{bot}^{n+1}\rho_{top}^{n+1} I_{sc}\left(h, t-\frac{2(n+1)h}{c}\right) \\ +c(\rho_{bot}-1)\,\rho_{bot}^{n}\rho_{top}^{n} I_{sc}\left(h, t-\frac{(2n+1)h}{c}\right) \end{bmatrix}. \tag{B2b}$$

If the risetime of injected lightning current is shorter than h/c, for $t < h/c$ all terms on the right-hand side of equation (B2b), except for the first term, are zero [*Bermudez et al.*, 2004]. Therefore we can rewrite equation (B2b) for $t < h/c$ as

$$E^{far}_{z\_tall}(d, t+d/c) = -\frac{1}{2\pi\varepsilon_0 c^2 d}\frac{\left(1-\rho_{top}\right)(c+v)}{2} I_{sc}(h,t). \tag{B3}$$

The far vertical electric field due to the same lightning strike to flat ground, calculated from equations (3) and (B1a) with $h = 0$ m, is given by

$$E^{far}_{z\_flat}(d, t+d/c) = -\frac{1}{2\pi\varepsilon_0 c^2 d}\frac{1+\rho_{gr}}{2} v I_{sc}(0,t). \tag{B4}$$

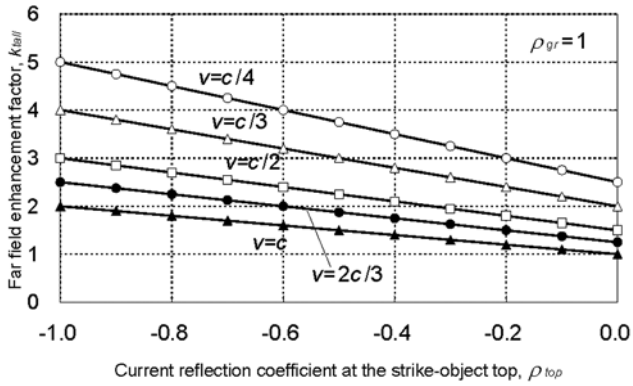

Figure B1. Far-field enhancement factor due to the presence of tall strike object as a function of ρ_{top} and v, calculated using equation (B5).

From equations (B3) and (B4), the far field enhancement factor due to the presence of tall strike object is given by

$$k_{tall} = \frac{E^{far}_{z\_tall}}{E^{far}_{z\_flat}} = \frac{\left(1-\rho_{top}\right)(c/v+1)}{\left(1+\rho_{gr}\right)} = \frac{v - v\rho_{top} + c\left(1-\rho_{top}\right)}{v+v\rho_{gr}}. \tag{B5}$$

Note that equation (B5) can be also obtained using far (essentially radiation) azimuthal magnetic fields. Equation (B5) shows clearly that far fields are larger for smaller values of ρ_{top}, ρ_{gr}, and v. Dependence of k_{tall} on ρ_{top} and v for $\rho_{gr} = 1$ is illustrated in Figure B1. For a realistic value of $\rho_{top} = -0.5$, as v varies from $c/4$ to c (the limiting value), k_{tall} varies from 3.8 to 1.5, respectively.

B2. Comparison With *Bermudez et al.*'s [2004] Far-Field Enhancement Factor

[67] Equation for far-field enhancement factor due to the presence of tall strike object derived for the transmission line (TL) model by *Bermudez et al.* [2004] is based on a distributed-shunt-current-source representation of the lightning channel proposed by *Rachidi et al.* [2002]. In this representation, shunt current sources distributed along the lightning channel are activated progressively when the return stroke wave front, propagating upward at speed v, arrives at their altitudes. The resultant partial current waves are assumed to propagate downward at the speed of light, c, and the upward waves reflected from ground or the top of strike object are also assumed to propagate along the channel at the speed of light, c.

[68] Vertical electric field equations, derived for the TL model in the same manner as equations (B3) and (B4) above but using equations (24), (25), and (3b) of *Rachidi et al.* [2002], are given by

$$E^{far}_{z\_tall}(d, t+d/c) = -\frac{1}{2\pi\varepsilon_0 c^2 d}\frac{v - c\rho_{top} + c\left(1-\rho_{top}\right)}{2} I_{sc}(h,t) \tag{B6}$$

$$E^{far}_{z\_flat}(d, t+d/c) = -\frac{1}{2\pi\varepsilon_0 c^2 d}\frac{v + c\rho_{gr}}{2} I_{sc}(0,t). \tag{B7}$$

Note that the equations of *Bermudez et al.* [2004] are written in terms of the so-called "undisturbed" (matched-conditions) current which is one half the short-circuit current, I_{sc}, used here. Equation (B6) is equivalent to equation (13) derived by *Bermudez et al.* [2004] for the tall-object case, while equation (B7) is different from equation (11) derived by *Bermudez et al.* [2004] for the flat-ground case. The latter can be obtained from equation (B7) by setting $\rho_{gr} = 0$. Note that equation (B7) is equivalent to equation (27) derived by *Bermudez et al.* [2004] for the flat-ground case with reflections from ground taken into account ($\rho_{gr} \neq 0$), although they did not use their equations (27) in deriving the far field enhancement factor.

[69] From equations (B6) and (B7), the far field enhancement factor due to the presence of tall strike object is given by

$$k'_{tall} = \frac{E^{far}_{z\_tall}}{E^{far}_{z\_flat}} = \frac{v - c\rho_{top} + c\left(1 - \rho_{top}\right)}{v + c\rho_{gr}}. \tag{B8}$$

Note that equation (B8), similar to equation (B5), gives the ratio of the fields normalized to the same charge transfer to ground.

[70] Equation for far-field enhancement factor due to the presence of tall strike object derived by *Bermudez et al.* [2004] is somewhat different and reproduced below.

$$k''_{tall} = \frac{v - c\rho_{top} + c\left(1 - \rho_{top}\right)}{v\left(1 - \rho_{top}\right)}. \tag{B9}$$

In this equation, $(1 - \rho_{top})$ in the denominator is the transmission coefficient at the top of the tower introduced by *Bermudez et al.* [2004] in their tall-object electric field equation, which is equivalent to our equation (B6), in order to express the field in terms of "measured" current. When the same "measured" current is used for the flat-ground case, as required in deriving the far-field enhancement factor equation, the same charge transfer to ground is assured only if $Z_{gr} = Z_{ob}$. However, it appears that in deriving equation (B9) Bermudez et al. implicitly assumed matched condition ($Z_{gr} = Z_{ch}$) at the channel base in the flat-ground case, which makes equation (B9) applicable only to the unrealistic situation when $Z_{gr} = Z_{ch} = Z_{ob}$, that is, $\rho_{gr} = \rho_{top} = 0$. Indeed, equations (B9) and (B8) converge to $(v + c)/v$ if $\rho_{gr} = \rho_{top} = 0$. For $v = 0.5c$, $\rho_{top} = -0.5$, $\rho_{gr} = 1$, equations (B8) and (B9) yield 1.7 and 3.3, respectively.

[71] We now compare equations (B8) and (B5). It is evident that the structure of equation (B8) is the same as that of equation (B5), and the difference between them is the speed: v versus c (in some of the terms). If one sets the speed of the current waves propagating along the lightning channel to v instead of c in equations (3b) and (24) of *Rachidi et al.* [2002], equation (B8) becomes identical to equation (B5). Also, equation (B8) is identical to equation (B5) in the unrealistic case of $\rho_{top} = \rho_{gr} = 0$. When $v = 0.5c$, $\rho_{top} = -0.5$, and $\rho_{gr} = 1$ (corresponding to $Z_{ch} = 3Z_{ob}$, $Z_{gr} = 0$), equations (B5) and (B8) yield similar values, 2.3 and 1.7, respectively.

[72] **Acknowledgments.** This research was supported in part by Doshisha University and by NSF grants ATM-0003994 and ATM-0346164. We would like to thank F. Rachidi, R. Thottappillil, M. A. Uman, and three anonymous reviewers for their valuable comments on the paper.

References

Baba, Y., and V. A. Rakov (2003), On the transmission line model for lightning return stroke representation, *Geophys. Res. Lett.*, *30*(24), 2294, doi:10.1029/2003GL018407.

Baba, Y., and V. A. Rakov (2005), On the use of lumped sources in lightning return stroke models, *J. Geophys. Res.*, *110*, D03101, doi:10.1029/2004JD005202.

Bermudez, J. L., F. Rachidi, W. Janischewskyj, V. Shostak, M. Rubinstein, A. M. Hussein, D. Pavanello, J. S. Chang, and M. Paolone (2004), Determination of lightning currents from far electromagnetic fields: Effect of a strike object, paper presented at 27th International Conference on Lightning Protection, Soc. de l'Electr., de l'Electron., et des Technol. de l'Inf. et de la Commun., Avignon, France.

Burke, G. J., and A. J. Poggio (1980), Numerical electromagnetic code (NEC)—Method of moments, *Tech. Doc. 116*, Naval Ocean Syst. Cent., San Diego, Calif.

Diendorfer, G., and W. Schulz (1998), Lightning incidence to elevated objects on mountains, paper presented at 24th International Conference on Lightning Protection, Natl. Lightning Safety Inst., Birmingham, UK.

Fisher, R. J., and G. H. Schnetzer (1994), 1993 triggered lightning test program: Environments within 20 meters of the lightning channel and small area temporary protection concepts, *Sandia Rep. SAND94-0311/UC-706*, Sandia Natl. Lab., Albuquerque, N. M.

Fuchs, F. (1998), On the transient behaviour of the telecommunication tower at the mountain Hoher Peissenberg, paper presented at 24th International Conference on Lightning Protection, Natl. Lightning Safety Inst., Birmingham, UK.

Janischewskyj, W., V. Shostak, J. Barratt, A. M. Hussein, R. Rusan, and J.-S. Chang (1996), Collection and use of lightning return stroke parameters taking into account characteristics of the struck object, paper presented at 23rd International Conference on Lightning Protection, Florence, Italy.

Kordi, B., R. Moini, and V. A. Rakov (2002), Comment on "Return stroke transmission line model for stroke speed near and equal that of light" by R. Thottappillil, J. Schoene, and M. A. Uman, *Geophys. Res. Lett.*, *29*(10), 1369, doi:10.1029/2001GL014602.

Kordi, B., R. Moini, W. Janischewskyj, A. M. Hussein, V. O. Shostak, and V. A. Rakov (2003), Application of the antenna theory model to a tall tower struck by lightning, *J. Geophys. Res.*, *108*(D17), 4542, doi:10.1029/2003JD003398.

Miyazaki, S., and M. Ishii (2004), Influence of elevated stricken object on lightning return-stroke current and associated fields, paper presented at 27th International Conference on Lightning Protection, Soc. de l'Electr., de l'Electron., et des Technol. de l'Inf. et de la Commun., Avignon, France.

Nucci, C. A., C. Mazzetti, F. Rachidi, and M. Ianoz (1988), On lightning return stroke models for LEMP calculations, paper presented at 19th International Conference on Lightning Protection, Assoc. of Austrian Electr. Eng. (OVE), Graz, Austria.

Nucci, C. A., G. Diendorfer, M. A. Uman, F. Rachidi, M. Ianoz, and C. Mazzetti (1990), Lightning return stroke current models with specified channel-base current: A review and comparison, *J. Geophys. Res.*, *95*(D12), 20,395–20,408.

Rachidi, F., W. Janischewskyj, A. M. Hussein, C. A. Nucci, S. Guerrieri, B. Kordi, and J.-C. Chang (2001), Current and electromagnetic field associated with lightning-return strokes to tall towers, *IEEE Trans. Electromagn. Compat.*, *43*(3), 356–367.

Rachidi, F., V. A. Rakov, C. A. Nucci, and J. L. Bermudez (2002), Effect of vertically extended strike object on the distribution of current along the lightning channel, *J. Geophys. Res.*, *107*(D23), 4699, doi:10.1029/2002JD002119.

Rakov, V. A. (2001), Transient response of a tall object to lightning, *IEEE Trans. Electromagn. Compat.*, *43*(4), 654–661.

Rakov, V. A. (2004), Lightning return stroke speed: A review of experimental data, paper presented at 27th International Conference on Lightning Protection, Soc. de l'Electr., de l'Electron., et des Technol. de l'Inf. et de la Commun., Avignon, France.

Rakov, V. A., R. Thottappillil, M. A. Uman, and P. P. Baker (1995), Mechanism of the lightning M component, *J. Geophys. Res.*, *100*(D12), 25,701–25,710.

Spiegel, M. R., and J. Liu (1998), *Schaum*'s *Mathematical Handbook of Formulas and Tables*, 2nd ed., McGraw-Hill, New York.

Thottappillil, R., and M. A. Uman (2002), Reply to the 'Comment on "Return stroke transmission line model for stroke speed near and equal

that of light" by R. Thottappillil, J. Schoene, and M. A. Uman' by B. Kordi, R. Moini, and V. A. Rakov, *Geophys. Res. Lett.*, *29*(10), 1505, doi:10.1029/2002GL014758.

Thottappillil, R., M. A. Uman, and V. A. Rakov (1998), Treatment of retardation effects in calculating the radiated electromagnetic fields from the lightning discharge, *J. Geophys. Res.*, *103*(D8), 9003–9013.

Thottappillil, R., J. Schoene, and M. A. Uman (2001), Return stroke transmission line model for stroke speed near and equal that of light, *Geophys. Res. Lett.*, *28*(18), 3593–3596.

Uman, M. A., D. K. McLain, and E. P. Krider (1975), The electromagnetic magnetic radiation from a finite antenna, *Am. J. Phys.*, *43*, 33–38.

Y. Baba, Department of Electrical Engineering, Doshisha University, Kyotanabe, Kyoto 610-0321, Japan. (ybaba@mail.doshisha.ac.jp)

V. A. Rakov, Department of Electrical and Computer Engineering, University of Florida, Gainesville, FL 32611, USA. (rakov@ece.ufl.edu)